

Temperature dependence and source apportionment of volatile organic compounds (VOCs) at an urban site on the north China plain

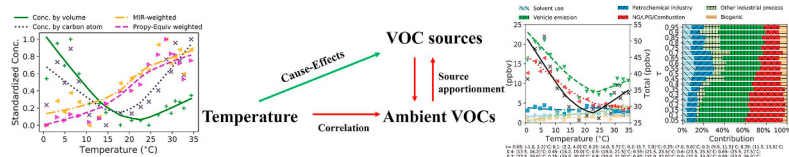
Congbo Song^{a,b}, Baoshuang Liu^a, Qili Dai^a, Huairui Li^b, Hongjun Mao^{a,b,*}

^a Center for Urban Transport Emission Research & State Environmental Protection Key Laboratory of Urban Ambient Air Particulate Matter Pollution Prevention and Control, College of Environmental Science and Engineering, Nankai University, Tianjin, 300071, China

^b Langfang Academy of Eco Industrialization for Wisdom Environment, Langfang, 065000, China



GRAPHICAL ABSTRACT



ARTICLE INFO

Keywords:
Volatile organic compounds
Temperature
Source apportionment
Cluster analysis
VOC reactivity
North China plain

ABSTRACT

Volatile organic compounds (VOCs) are largely affected by ambient temperature. However, responses of source-specific VOCs to ambient temperature are poorly understood. Based on one-year (2016.4–2017.3) observations for 57 VOC species (average: 33.4 ± 26 ppbv), and on the use of a *k*-means cluster technique and positive matrix factorization model, temperature dependence of VOCs and their potential sources were studied. The VOC reactivity was dominated by alkenes, though alkanes contributed the most to the VOCs both by volume and by carbon atoms. The cluster analysis suggested that real-world VOCs were influenced directly and indirectly by temperature. The responses of the VOCs in terms of volume and carbon atoms to temperature exhibited V-shape patterns, and the inflection points occurred when temperatures were around 15–25°C. Nevertheless, the VOC reactivity generally increased with increasing temperature, suggesting that temperature could be used as a proxy for VOC reactivity. The source apportionment study revealed that vehicle emissions (44.8%) contributed the most to ambient VOCs, and followed by natural gas (NG)/liquefied petroleum gas (LPG)/Combustion (24.9%), petrochemical industry (9.6%), other industrial process (8.4%), solvent use (7.4%), and biogenic emission (4.9%). Solvent use and biogenic emissions were the greatest contributors to VOC reactivity. Unexpectedly high propane/ethylene ratios were observed at low temperatures. This might be associated with domestic heating-related emissions from NG/LPG sources because their contributions generally increased with the decreasing temperature. By comparison with ~25 °C, the VOC concentrations and ozone formation potentials contributed by vehicles were respectively 7- and 2.6-times greater at ~0 °C (cold engine starts dominance), and were 50.4% and 57.5% greater at ~35 °C (gasoline evaporation dominance). Local emission controls for VOCs were beneficial for alleviating atmospheric secondary pollution because the potential source-areas of VOCs were mostly distributed in the geographically flat North China Plain. However, alkanes-dominated VOC sources (e.g., vehicle emission, NG/LPG) could experience long-distance air transport because of their relatively long atmospheric lifetime. The results highlight that the temperature dependences of VOCs depend on the emission sources, and this is of great value in understanding the linkage between meteorology and air quality.

* Corresponding author. College of Environmental Science and Engineering, Nankai University, Tianjin, 300071, China.
E-mail addresses: songcongbo@163.com (C. Song), hongjunm@nankai.edu.cn (H. Mao).

1. Introduction

In recent years, the North China Plain (NCP) has been frequently experienced both photochemical pollution (Ma et al., 2016) and haze-fog episodes (Guo et al., 2014; Sun et al., 2014) due to high emission of precursors and the presence of geographically flat plains (Zhao et al., 2009). Volatile organic compounds (VOCs), precursors contributing to formation of secondary organic aerosol (SOA) and tropospheric ozone (O_3), have been given a large amount of attentions in China. Determination of VOC emissions from various sources (biogenic and anthropogenic) is essential to further our understanding of their impacts on urban air quality and public health. In urban areas, VOC emissions are generally dominated by anthropogenic sources, including industry, solvent use, residential, transportation, and power sector (Li et al., 2017). The VOC emissions are largely driven by ambient temperature because of their vapor pressures, human activities, and photochemical reactions. Compared to the temperature dependence of organic reactivities (Arrhenius in form) (Pusede et al., 2015, 2014), the temperature dependence of VOCs (primarily driven by emissions) is generally missed in emission inventories in the regional and global chemical transport models, which leads to important uncertainties in accurate reproduction of air quality by modelling. Ambient temperature is reported to be associated with NO_x from soil (Romer et al., 2018) and power plants (Abel et al., 2017) emissions, and associated with VOCs from biogenic emissions (Fu et al., 2015; Steiner et al., 2010), evaporative emissions (Rubin et al., 2006), tailpipe emissions (George et al., 2017, 2015), and fugitive emissions from petroleum operations (Gentner et al., 2014). These studies reveal that both the biogenic emissions and anthropogenic emissions are directly and indirectly related to the ambient temperature.

However, it would not have been possible to directly measure the responses of source-specific VOC emissions to the ambient temperature because the responses could be largely affected by temperature-driven human activities in addition to the laws of nature. Pusede et al. (2014) categorized the VOC reactivity as either temperature independent or temperature dependent, and reported the responses of daily average VOC reactivity of species by source category to daily maximum temperature. However, the ambient VOCs are well mixed from multiple sources, and the linkage between temperature and anthropogenic VOC sources is still not well understood. Receptor models can be utilized to quantify responses of source-specific VOCs to temperature because the receptor can detect signatures of changes in emission sources. Although multiple studies on source apportionment of ambient VOCs have been performed in major cities on the NCP (Gao et al., 2018; Wang et al., 2016; Liu et al., 2016; Han et al., 2015; Song et al., 2007), few studies have investigated the linkage between temperature and emission sources of VOCs. Furthermore, the air quality in Langfang can be profoundly influenced by megacities such as Beijing and Tianjin. However, few studies reported source apportionments and geographic origins of VOCs in medium cities in the most polluted part of the NCP. Langfang city has a large number of emission sources of VOCs, including motor vehicles, machinery and electronics, food industry, new building materials, light industrial textiles and bio-pharmaceutical industries. According to the 'Bulletin of the Chinese Ecological Environment' in 2014, 2015, and 2016, the air quality in Langfang ranked third, ninth, and twelfth, respectively, from the bottom among the 74 leading cities of China. Study on the characteristics and potential sources of ambient VOCs in Langfang, one of the most polluted cities on the NCP, is helpful for development of effective abatement strategies for ambient VOCs in median cities in the region.

In the present study, one year of continuous measurement of VOCs was carried out to analyze the temperature dependence and source apportionment of VOCs in urban Langfang. Cluster analysis was conducted to classify the responses of VOC concentrations to temperature. The positive matrix factorization (PMF) model, a widely used receptor model, was employed to identify and apportion the possible sources of

ambient VOCs. Base on the results of the source apportionment, the responses of source-specific VOCs to temperature were further studied. The potential source-areas of source-specific VOCs were also investigated to reveal implications of an emission control strategy. Results from this study provided direct observations of the temperature dependence of VOCs and their potential sources, and enhanced our understanding of source-specific VOC emissions for more reliable emission inventory, air quality modelling, secondary pollution, emission control strategies, and health effect studies.

2. Materials and methods

2.1. Site and measurements

From April 2016 to March 2017, continuous measurement of VOCs using online instruments was carried out at the atmospheric monitoring site (116°45'42'', 39°34'18''), located on the rooftop of a nine-story building in the northeast of Langfang city. As shown in Fig. 1, Langfang city is a medium-size city located between the two largest megacities in China: Beijing and Tianjin. With few local pollutant sources within 2–3 km surroundings of the site, it can be considered as an urban site in the most polluted part of the NCP.

The VOCs were continuously monitored at 1 h sampling intervals using a GC955 series 611/811 VOC analyzer, from Syntech Spectras Inc., Holland. The 57 VOC species (including alkanes, alkenes, alkyne, and aromatics) designated as photochemical precursors by the United States Environmental Protection Agency (US EPA) were used for the equipment calibration before monitoring, were then analyzed. The analyses were done using a photo ionization detector (PID) and a flame ionization detector (FID), which ensured high sensitivity and good identification. The GC955 series 611 and 811 are two separate sample systems and column systems, which measure low boiling point VOCs species (C2–C5 VOCs) and high boiling point VOCs species (C6–C12 VOCs), respectively. For the GC955 series 611 analyzer, hydrocarbons are preconcentrated on Carbosieves S111 at 5°C, desorbed thermally and separated on a combination of two columns: a capillary film column and a capillary PLOT column. In this way, the low boiling hydrocarbons can be separated. For the GC955 series 811 analyzer, hydrocarbons are preconcentrated on Tenax GR, desorbed thermally, and then separated on the EPA624 equivalent column, to achieve optimal separation from interfering hydrocarbons. Zero and span gas checks were conducted monthly using the 5-point method, and the correlation coefficient usually varied from 0.995 to 0.999. The method detection limits (MDLs) and detectors for each VOC species are listed in Table S1. The temperature data were simultaneously measured using a VAISALA WXT520 (Helsinki, Finland) automatic weather station.

2.2. Chemical reactivity of VOCs

To understand the effects of VOCs on O_3 formation potentials (OFPs), the kinetic reactivity and mechanism reactivity of the VOCs were determined (Liu et al., 2016; Zou et al., 2015; Chameides et al., 1992). The kinetic reactivity of the VOCs was estimated by their propylene-equivalent (Propy-Equiv) concentrations.

$$C_{j, \text{Propy-Equiv}} = C_{j, \text{ppbC}} \times \frac{k_{j, OH}}{k_{\text{Propy}, OH}} \quad (1)$$

where j is a VOC species, $C_{j, \text{ppbC}}$ represents the carbon atom concentration (ppbC) of the species, and $k_{j, OH}$ and $k_{\text{Propy}, OH}$ represent the chemical reaction rate constants in the free radical reaction of species j and propylene with OH, respectively. $k_{j, OH}$ was obtained from Atkinson and Arey (2003).

The mechanism reactivity of the VOCs was estimated by their maximum-incremental-reactivity (MIR) weighted concentrations (the maximum concentration of O_3 generated by the species in terms of

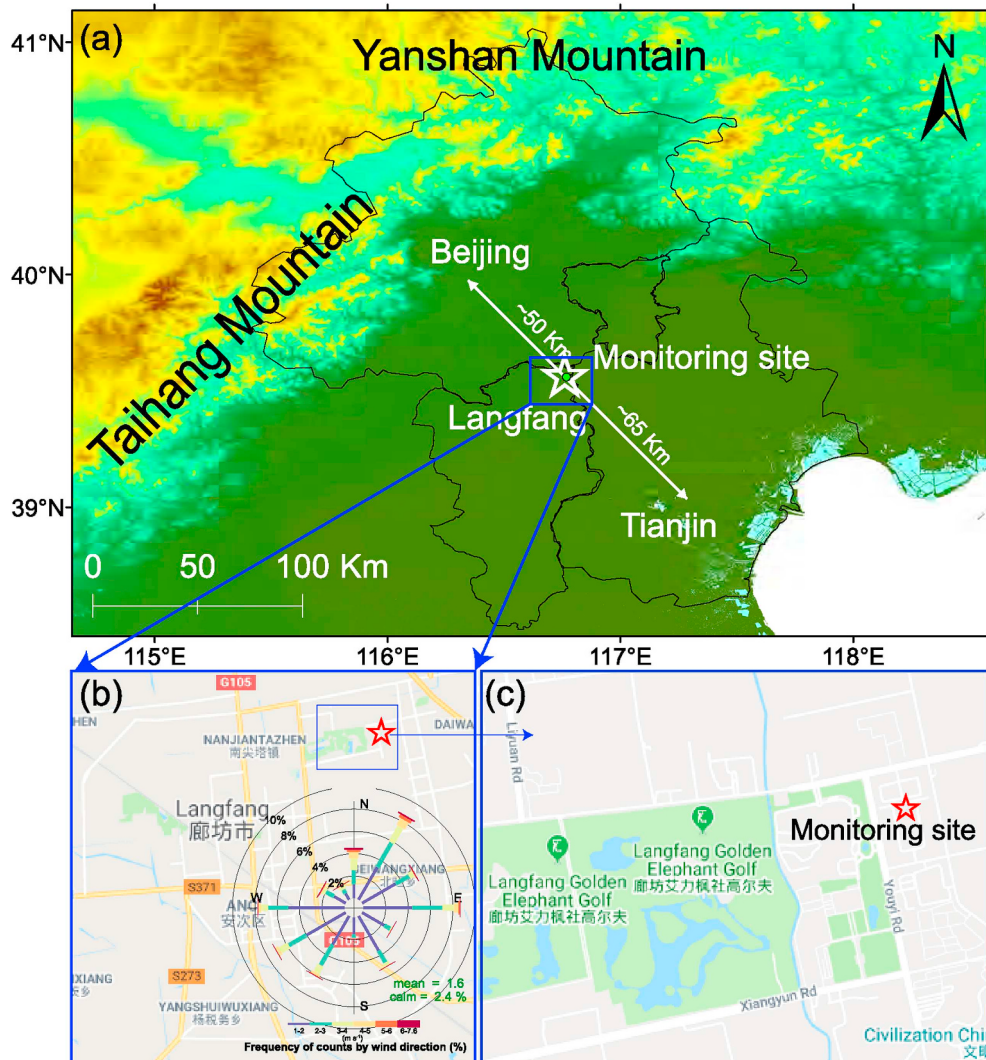


Fig. 1. Geographical information of the monitoring site (denoted as a star between Beijing and Tianjin), which is located on the rooftop of a nine-story building in the northeast of Langfang city, between the megacities of Beijing and Tianjin on the North China Plain.

estimated MIR).

$$C_{j,MIR} = MIR_j \times C_{j,ppbv} \times \frac{m_j}{M} \quad (2)$$

where $C_{j,ppbv}$ represents the actual concentration by volume (ppbv) for species j , m_j and M represents the molecular mass of species j and O_3 , respectively. The MIR_j was estimated by selecting the specific MIR value for each VOC species from published studies (Carter, 1994; Dodge, 1984).

2.3. Cluster analysis

To investigate the relationship between VOCs and ambient temperature, cluster analysis was used to classify patterns of responses of VOCs to temperature into several groups with comparable values and similar variation trends within groups. The k -means clustering algorithm (package) available in R software (version 3.4.2) was used in this study. The k -means clustering technique divided the multi-dimensional data into a predefined number of subgroups, which were as different as possible from each other, but as coincident as possible within themselves. This was done by iteratively minimizing the sum of squared Euclidean distances from each member to its cluster centroid (Zhao et al., 2019, 2016).

Since the average concentrations varied greatly among different VOC species, the concentrations of each compound under different

temperature sections (cut by 19 quantiles, from 0.05 to 0.95 for every 0.05 quantile) were preprocessed using min-max normalization:

$$y_i = \frac{x_i - \min_{1 \leq j \leq n} \{x_j\}}{\max_{1 \leq j \leq n} \{x_j\} - \min_{1 \leq j \leq n} \{x_j\}} \quad (3)$$

where x and y were the absolute and standardized concentrations, respectively. The subscript i and j denoted temperature sections. n was the number of temperature sections (i.e., 19 in this study).

Then standardized concentrations were clustered by k -means. The determination of the most appropriate number of clusters, a very complicated and important problem, was conducted by the R package NbClust (Charrad et al., 2014) in the present study based on multiple statistical rules (e.g., Elbow method, Silhouette method, and Gap statistic method, see the supplementary file). Further detailed information regarding the optimal number of k -means clusters is given in the supplementary file (Figs. S1–S2).

2.4. PMF analysis

EPA PMF 5.0 was used to identify and apportion the possible sources of ambient VOCs. PMF is an advanced receptor model that decomposes a matrix of sample data (X) into two matrices, the source

contribution matrix (G) and the source matrix (F), based on observations at the sampling site. The PMF model can be expressed as follows (Paatero and Tapper, 1994; Paatero, 1997):

$$X_{ij} = \sum_{k=1}^p g_{ik} f_{kj} + e_{ij} \quad (4)$$

where, X_{ij} is the j th compound concentration of the i th sample, g_{ik} is the contribution of the k th source to the i th sample, f_{kj} is the source profile of the j th compound in the k th source, e_{ij} is the residual matrix for the j th compound in the i th sample, and p is the total number of independent sources.

The parameters (g_{ik} and f_{kj}) are constrained to nonnegative values. The task of PMF is to calculate the minimum value Q , as follows:

$$Q(E) = \sum_{i=1}^n \sum_{j=1}^m \left(\frac{e_{ij}}{\sigma_{ij}} \right)^2 \quad (5)$$

where, σ_{ij} is the uncertainty in the j th compound for the i th sample.

The uncertainties of the input datasets were calculated using Equations (6) and (7). If the VOC concentration (Conc.) is less than MDL, Equation (6) is adopted. Otherwise, Equation (7) is adopted.

$$Unc = \frac{5}{6} \times MDL \quad (6)$$

$$Unc = \sqrt{(ErrorFraction \times Conc.)^2 + (0.5 \times MDL)^2} \quad (7)$$

where MDL represents the detection limit, and the Error Fraction can be set to 5%–20% depending on the concentration (Hui et al., 2018; Song et al., 2007). The Error Fraction in this study was set to 10% by experience (Liu et al., 2017).

The appropriate species for the PMF model were determined following some basic criteria: (1) species for which the data loss is more than 25% or for which concentrations below MDL are more than 35%, are excluded; (2) species that are highly reactive should be excluded because they rapidly react away in the atmosphere; and (3) species that are source identification species are retained. Finally, 21 VOC species were selected to include in the PMF analysis (Fig. 4), because they were either the most abundant species or were source identification species (Zheng et al., 2018; Liu et al., 2016). The six-factor solution was determined to be the optimal solution in the PMF analysis based on: (1) principal component analysis of the VOC data; (2) field survey-based VOC emission inventory of the study area; and (3) Q_{true} / Q_{except} for different factor numbers in the PMF (see the supplementary file, Figs. S3–S4 and Tables S2–S3).

2.5. Backward trajectory and PSCF model

In this study, the 24-h air mass backward trajectory arriving at the monitoring site was calculated at 1-h intervals from April 2016 to March 2017 using the Hybrid Single-Particle Lagrangian Integrated Trajectory (HYSPLIT) model developed by the National Oceanic and Atmospheric Administration (NOAA). The arrival height was set at 100 m above the ground level (Liu et al., 2018, 2016). The final global analysis data produced by the National Center for Environmental Prediction's Global Data Assimilation System (GDAS) wind field reanalysis were introduced into the trajectory calculation. A total of 8736 backward trajectories were generated and then grouped into four clusters according to their geographic sources and histories (see Fig. S5).

The potential source contribution function (PSCF) values were calculated to identify the potential geographic origins of VOCs using the source contributions apportioned from the PMF model and the backward trajectory (Zheng et al., 2018). The study region (covered by over 95% of the backward trajectories (i.e., 31–58°N, 85–126°E) was divided into $x \times y$ small, equal grid cells, with a resolution of 0.5° × 0.5°. The PSCF value is defined with Equation (8):

$$PSCF_{i,j} = \frac{m_{i,j}}{n_{i,j}} \quad (8)$$

where i and j are the latitude and longitude, $n_{i,j}$ is the total number of endpoints that fall in the i, j th cell, and $m_{i,j}$ is defined as the number of endpoints in the same cell that exceed the threshold criterion. The 75th percentile of each identified source contribution was used as the criterion value. When $n_{i,j}$ was smaller than 3-times the grid average number of the trajectory endpoint (in this case, $n_{ave} = 50$), the uncertainty of the cell was reduced by multiplying a weight function ($W_{i,j}$) into the PSCF value. The weight function can be calculated using the equations below:

$$WPSCF = \frac{m_{i,j}}{n_{i,j}} \times W(n_{i,j}) \quad (9)$$

$$W(n_{i,j}) = \begin{cases} 1.00, & 3n_{ave} < n_{i,j} \\ 0.70, & 1.5n_{ave} < n_{i,j} \leq 3n_{ave} \\ 0.42, & n_{ave} < n_{i,j} \leq 1.5n_{ave} \\ 0.20, & n_{i,j} \leq n_{ave} \end{cases} \quad (10)$$

The trajectory clustering and PSCF analysis were conducted using the GIS-based software TrajStat (Wang et al., 2009).

3. Results and discussion

3.1. General characteristics of VOCs

Table 1 shows the average values (mean ± standard deviation) of the VOC concentrations (Conc.) based on different scales, and the annual average concentrations of the total VOCs were 33.4 ± 26 ppbv for the concentration by volume, 126.4 ± 88.4 ppbC for the concentration by carbon atoms, 85 ± 50 ppbv for the MIR-weighted concentration, and 44.5 ± 32 ppbC for the Propy-Equiv concentration. **Table 2** presents a comparison of VOC compositions between this study and previous studies in China and other countries (Zhu et al., 2018; Hui et al., 2018; Liu et al., 2016; Jia et al., 2016; Li et al., 2015; Garzn et al., 2015; An et al., 2014; Wang et al., 2013; Leuchner and Rappenglück, 2010; Na and Kim, 2001). The annual average concentration of the VOCs in Langfang was higher than that in Beijing (23.4 ppbv), Shanghai (27.7 ppv), Wuhan (25.7 ppbv), Gucheng (23.6 ppbv), and Quzhou (15.5 ppbv). It was similar to that in Tianjin (28.7 ppbv), Zhengzhou (29.2 ppbv), Lanzhou (38.3 ppbv), and Houston (31.2 ppbv), but lower than that in the Mid-lower Yangtze River (49.9 ± 8.9 ppbv), Nanjing (43.5 ppbv), Souel (121.8), and Mexico (84.0 ppbv). Alkanes constituted the largest proportion of the VOCs both by volume (22.9 ± 19.1 ppbv, 66.2 ± 12.4%) and by carbon atoms (87.3 ± 69.2 ppbC, 65.5 ± 13.0%), which was consistent with a previous study in Tianjin (Liu et al., 2016). Alkenes accounted for < 15% of the VOCs both by volume and carbon atoms, but contributed the most to VOC reactivity, and were responsible for 45.6 ± 17.9% and 50.0 ± 21.3% of the MIR-weighted and the Propy-Equiv concentrations, respectively. Alkenes and aromatics have been also recognized as the most important contributors to OFPs in Chinese megacities (alkenes: Beijing (Gao et al., 2018), Tianjin (Liu et al., 2016), Nanjing (Shao et al., 2016), Chongqing (Li et al., 2018), and Chengdu (Deng et al., 2019); aromatics: Shanghai (Wang et al., 2013), and Guangzhou (Zou et al., 2015)).

By comparison, the fraction of alkanes in Langfang (67.1%) was higher than that in other cities (Beijing: 59.1%; Tianjin: 59.1%; Zhengzhou 56.7%; Wuhan: 61.9%; Nanjing: 45.1%; Gucheng: 56.1%; Quzhou: 56.8%; Shanghai: 46.2%; Lanzhou: 57.0%; Souel: 45.3%; and Mexico: 63.0%). Meanwhile, the fraction of alkynes in this study (14.4%) was also higher than that in other cities (Beijing: 9.4%; Wuhan: 9.3%; Nanjing: 7.3%; Gucheng: 10.2%; Quzhou: 12.6%; Shanghai: 9.4%; Lanzhou: 57.0%; Houston: 4.1%; and Mexico: 6.2%). Accordingly, the fractions of alkenes (10.9%) and aromatics (7.6%) in

Table 1

Average values (mean \pm standard deviation) of the VOC concentrations (Conc.) by volume and carbon atoms, the MIR-weighted concentrations, and the Propy-Equiv concentrations of the measured species in the ambient air of Langfang (from April 2016 to March 2017). The bold indicates that the average concentration is in the top 10.

Compound	Conc. by volume	Conc. by carbon atoms	MIR-weighted	Propy-Equiv weighted
	(ppbv)	(ppbC)	(ppbv)	(ppbC)
Ethane	6.83 \pm 7.5	13.66 \pm 14.99	1.11 \pm 1.22	0.14 \pm 0.15
Propane	7.05 \pm 6.55	21.14 \pm 19.64	2.98 \pm 2.77	0.92 \pm 0.86
n-Butane	1.53 \pm 1.41	6.12 \pm 5.62	2 \pm 1.84	0.59 \pm 0.54
<i>i</i> -Butane	2.56 \pm 2.62	10.26 \pm 10.47	3.66 \pm 3.74	0.91 \pm 0.93
n-Pentane	0.64 \pm 0.54	3.21 \pm 2.7	1.18 \pm 0.99	0.48 \pm 0.41
Cyclopentane	2.08 \pm 6.88	10.39 \pm 34.41	6.8 \pm 22.52	2.04 \pm 6.75
<i>i</i> -Pentane	1.28 \pm 1.08	6.42 \pm 5.41	2.62 \pm 2.21	0.95 \pm 0.8
n-Hexane	0.17 \pm 0.17	1.05 \pm 1.02	0.36 \pm 0.35	0.21 \pm 0.2
2,2-Dimethylbutane	0.19 \pm 0.44	1.15 \pm 2.67	0.38 \pm 0.89	0.1 \pm 0.24
2,3-Dimethylbutane	0.46 \pm 0.79	2.78 \pm 4.73	0.75 \pm 1.27	0.67 \pm 1.13
2-Methylpentane	1.16 \pm 0.95	6.98 \pm 5.68	2.92 \pm 2.38	1.49 \pm 1.21
3-Methylpentane	0.07 \pm 0.06	0.4 \pm 0.35	0.2 \pm 0.18	0.09 \pm 0.08
Methylcyclopentane	0.31 \pm 0.54	1.89 \pm 3.25	1.13 \pm 1.95	0.37 \pm 0.63
Cyclohexane	0.08 \pm 0.09	0.47 \pm 0.52	0.16 \pm 0.17	0.13 \pm 0.15
n-Heptane	0.1 \pm 0.09	0.7 \pm 0.6	0.2 \pm 0.17	0.19 \pm 0.16
2,3-Dimethylpentane	0.04 \pm 0.04	0.25 \pm 0.3	0.09 \pm 0.11	0.05 \pm 0.06
2,4-Dimethylpentane	0.03 \pm 0.04	0.22 \pm 0.26	0.09 \pm 0.11	0.05 \pm 0.06
2-Methylhexane	0.06 \pm 0.07	0.4 \pm 0.46	0.13 \pm 0.15	0.1 \pm 0.12
3-Methylhexane	0.08 \pm 0.08	0.53 \pm 0.56	0.24 \pm 0.25	0.1 \pm 0.11
Methylcyclohexane	0.01 \pm 0.02	0.08 \pm 0.12	0.03 \pm 0.05	0.03 \pm 0.05
n-Octane	0.06 \pm 0.05	0.49 \pm 0.41	0.12 \pm 0.1	0.16 \pm 0.14
2-Methylheptane	0.01 \pm 0.01	0.06 \pm 0.08	0.02 \pm 0.02	0.02 \pm 0.03
3-Methylheptane	0.01 \pm 0.02	0.11 \pm 0.19	0.04 \pm 0.06	0.04 \pm 0.06
2,2,4-Trimethylpentane	0.05 \pm 0.07	0.42 \pm 0.54	0.15 \pm 0.19	0.06 \pm 0.08
2,3,4-Trimethylpentane	0.05 \pm 0.05	0.38 \pm 0.43	0.11 \pm 0.12	0.09 \pm 0.11
n-Nonane	0.06 \pm 0.05	0.55 \pm 0.47	0.11 \pm 0.09	0.21 \pm 0.18
n-Decane	0.05 \pm 0.03	0.46 \pm 0.31	0.08 \pm 0.05	0.2 \pm 0.14
n-Undecane	0.04 \pm 0.05	0.39 \pm 0.53	0.06 \pm 0.08	0.2 \pm 0.27
n-Dodecane	0.04 \pm 0.05	0.39 \pm 0.53	0.06 \pm 0.08	0.2 \pm 0.27
Acetylene	4.91 \pm 5.7	9.82 \pm 11.41	2.53 \pm 2.94	1.61 \pm 1.87
Ethylene	1.25 \pm 0.92	2.49 \pm 1.85	6.47 \pm 4.8	0.81 \pm 0.6
Propylene	0.68 \pm 0.45	2.04 \pm 1.34	6.88 \pm 4.54	2.04 \pm 1.34
1-Butene	0.72 \pm 0.76	2.89 \pm 3.05	8.09 \pm 8.54	3.46 \pm 3.65
<i>cis</i> -2-Butene	0.23 \pm 0.44	0.93 \pm 1.74	3.86 \pm 7.25	1.99 \pm 3.73
<i>trans</i> -2-Butene	0.21 \pm 0.38	0.86 \pm 1.53	3.82 \pm 6.81	2.09 \pm 3.73
1,3-Butadiene	0.58 \pm 1.88	2.31 \pm 7.52	5.92 \pm 19.25	5.85 \pm 19.04
1-Pentene	0.1 \pm 0.08	0.52 \pm 0.39	1.08 \pm 0.81	0.62 \pm 0.47
<i>cis</i> -2-Pentene	0.04 \pm 0.09	0.22 \pm 0.44	0.67 \pm 1.32	0.55 \pm 1.09
<i>trans</i> -2-Pentene	0.04 \pm 0.04	0.18 \pm 0.18	0.54 \pm 0.55	0.45 \pm 0.46
Isoprene	0.69 \pm 0.74	3.44 \pm 3.69	10.22 \pm 10.98	13.2 \pm 14.18
1-Hexene	0.02 \pm 0.05	0.15 \pm 0.28	0.23 \pm 0.44	0.21 \pm 0.4
Benzene	0.86 \pm 0.63	5.14 \pm 3.79	0.96 \pm 0.71	0.24 \pm 0.18
Toluene	0.84 \pm 0.63	5.91 \pm 4.42	6.37 \pm 4.77	1.34 \pm 1
Styrene	0.05 \pm 0.06	0.38 \pm 0.45	0.17 \pm 0.2	0.84 \pm 0.99
Ethylbenzene	0.35 \pm 0.31	2.77 \pm 2.45	2.27 \pm 2	0.73 \pm 0.65
<i>m, p</i> -Xylene	0.34 \pm 0.33	2.76 \pm 2.66	7.42 \pm 7.17	2.15 \pm 2.08
<i>o</i> -Xylene	0.28 \pm 0.28	2.26 \pm 2.27	4.73 \pm 4.76	1.17 \pm 1.17
<i>i</i> -Propylbenzene	0 \pm 0.01	0.04 \pm 0.06	0.03 \pm 0.04	0.01 \pm 0.02
n-Propylbenzene	0.01 \pm 0.01	0.09 \pm 0.13	0.05 \pm 0.07	0.02 \pm 0.03
1,2,3-Trimethylbenzene	0.02 \pm 0.01	0.2 \pm 0.09	0.66 \pm 0.31	0.25 \pm 0.12
1,2,4-Trimethylbenzene	0.04 \pm 0.03	0.38 \pm 0.31	0.95 \pm 0.76	0.48 \pm 0.38
1,3,5-Trimethylbenzene	0.02 \pm 0.01	0.2 \pm 0.11	0.64 \pm 0.37	0.42 \pm 0.24
<i>m</i> -Ethyltoluene	0.02 \pm 0.02	0.17 \pm 0.22	0.34 \pm 0.46	0.12 \pm 0.16
<i>p</i> -Ethyltoluene	0.01 \pm 0.01	0.09 \pm 0.13	0.11 \pm 0.16	0.04 \pm 0.06
<i>o</i> -Ethyltoluene	0.01 \pm 0.01	0.13 \pm 0.13	0.2 \pm 0.2	0.06 \pm 0.06
<i>m</i> -Diethylbenzene	0.01 \pm 0.01	0.08 \pm 0.13	0.16 \pm 0.25	0.04 \pm 0.07
<i>p</i> -Diethylbenzene	0.01 \pm 0.01	0.06 \pm 0.13	0.07 \pm 0.16	0.02 \pm 0.05
Alkanes	22.93 \pm 19.15	87.25 \pm 69.22	24.09 \pm 24.18	13.67 \pm 17.12
Alkenes	3.7 \pm 2.72	12.67 \pm 9.87	38.35 \pm 27.98	23.3 \pm 23.26
Alkyne	4.91 \pm 5.7	9.82 \pm 11.41	2.53 \pm 2.94	1.61 \pm 1.87
Aromatics	2.56 \pm 1.85	18.09 \pm 13.31	20.37 \pm 17.54	6.2 \pm 5.41
VOCs	33.38 \pm 26.03	126.4 \pm 88.38	84.97 \pm 49.99	44.53 \pm 32.02

Langfang were lower than those in other cities. As shown in Table 2, alkanes were likely to be the most abundant species among VOCs in Chinese major cities during the last few years. The high-content alkanes and alkynes in the VOCs in Langfang might be associated with high

demand for fuel combustion in the Beijing-Tianjin-Hebei region.

The top ten most abundant species (see Table 1) measured in this study were propane (7 ppbv), ethane (6.8 ppbv), acetylene (4.9 ppbv), *i*-butane (2.6 ppbv), cyclopentane (2.1 ppbv), n-butane (1.5 ppbv), *i*-

Table 2

Comparisons of VOC levels and their compositions in Langfang and other cities in China and other countries.

	(Conc./ppbv, Percentage in VOCs)				VOCs*/ppbv
	Alkanes	Alkenes	Alkyne	Aromatics	
Langfang (2016.4–2017.3) ^a	(22.9 ± 19.1, 67.1%)	(3.7 ± 2.7, 10.9%)	(4.9 ± 5.7, 14.4%)	(2.6 ± 1.8, 7.6%)	33.4 ± 26
Beijing (2013–2014) ^b	(13.5, 59.1%)	(3.8, 15.9%)	(2.2, 9.4%)	(3.9, 15.5)	23.4
Tianjin (2014.11–2015.10) ^c	(18.3, 62.5%)	(5.2, 17.7%)	N.A.	(5.9, 20.1%)	28.7
Zhengzhou (2017.5–2017.9) ^d	(16.6, 56.7%)	(4.7, 16.2%)	(3.8, 12.9%)	(4.1, 14.1%)	29.2
Wuhan (2016.9–2017.8) ^e	(15.9, 61.9%)	(4.2, 16.3%)	(2.4, 9.3%)	(3.2, 12.5%)	25.7
Mid-lower Yangtze River (2015) ^f	(26.4 ± 7.2, 40.3%)	(11.3 ± 3.6, 17.2%)	(5.9 ± 2.7, 9.1%)	(6.3 ± 2.6, 9.5%)	49.9 ± 8.9
Nanjing (2011.3–2012.2) ^g	(19.6, 45.1%)	(11.1, 25.3%)	(3.2, 7.3%)	(9.7, 22.3%)	43.5
Gucheng (2013–2014) ^h	(13.3, 56.1%)	(4.8, 19.8%)	(1.9, 10.2%)	(3.6, 13.9%)	23.6
Quzhou (2013–2014) ⁱ	(8.8, 56.8%)	(3.0, 19.2%)	(1.9, 12.6%)	(1.8, 11.4%)	15.5
Shanghai (2009.1–2010.12) ^j	(12.8, 46.2%)	(3.6, 13.0%)	(2.6, 9.4%)	(8.7, 31.4%)	27.7
Lanzhou (2013.6–2013.8) ^k	(21.9, 57.0%)	(7.7, 20.2%)	N.A.	(8.7, 22.8%)	38.3
Souel (1998.8–1999.7) ^l	(55.2, 45.3%)	(8.3, 6.8%)	N.A.	(58.3, 47.9%)	121.8
Houston (2006.8–2006.9) ^m	(24.2, 74.4%)	(4.2, 12.8%)	(1.3, 4.1%)	(2.8, 8.7%)	31.2
Mexico (2011–2012) ⁿ	(52.9, 63.0%)	(12.4, 14.8%)	(5.2, 6.2%)	(13.4, 15.9%)	84.0

Superscript: a: Langfang, this study; b: Beijing (Li et al., 2015); c: Tianjin (Liu et al., 2016); d: Zhengzhou (Li et al., 2019); e: Wuhan (Hui et al., 2018); f: Mid-lower Yangtze River (Zhu et al., 2018); g: Nanjing (An et al., 2014); h: Gucheng (Li et al., 2015); i: Quzhou (Li et al., 2015); j: Shanghai (Wang et al., 2013); k: Lanzhou (Jia et al., 2016); l: Souel (Na and Kim, 2001); m: Houston (Leuchner and Rappenglück, 2010); n: Mexico (Garzn et al., 2015).

N.A.: data not available.

*: VOCs denote the sum of PAMS (photochemical assessment monitoring stations) species.

pentane (1.3 ppbv), 3-methylpentane (1.2 ppbv), ethylene (1.2 ppbv), and benzene (0.9 ppbv). The high fractions of propane and ethane could be attributed to both the associated anthropogenic emissions and to their relatively long atmospheric lifetimes (47 days for ethane and 10.5 days for propane) (Jobson et al., 1998). Isoprene, accounting for about half of the total BVOCs, contributed the most to both the MIR-weighted (11 ± 10.9%) and the Propy-Equiv (22.7 ± 19%) concentrations, which suggested that biogenic emissions need to be considered because of their high OFP and OH reactivities, aside from the anthropogenic VOC emissions. Zong et al. (2018) also demonstrated the significant mixed effects of both anthropogenic pollution from urban zones and biogenic emissions in rural areas on the regional O₃ pollution in the NCP region.

3.2. Temperature dependence of VOCs

The observed VOCs can be broadly categorized as either temperature independent or temperature dependent. Pusede et al. (2014) reported that the daily average VOC reactivity of certain anthropogenic VOCs is independent of temperature. The known BVOCs and a subset of alkanes increase exponentially with increase of the temperature. Moreover, the observed temperature dependence is driven primarily by temperature effects on VOC concentrations (presumably emissions) rather than by acceleration of the OH reaction rates. In this study, the k-means clustering technique was used to classify the responses of VOC species to ambient temperature, and three clusters (Cluster 1, Cluster 2, and Cluster 3) were determined (Fig. 2a). The VOC species that appeared in each cluster are given in Fig. 2b.

The VOC concentrations for Cluster 1 and Cluster 2 (see Fig. 2a) monotonically decrease and increase with temperature, respectively. Meanwhile, the VOC concentrations for Cluster 3 increase and decrease with temperature when temperatures was lower and higher, respectively, than ~25°C. For ethane, propane, acetylene, isopentane, *i*-butane, and *n*-butane, the key markers for natural gas (NG)/liquefied petroleum gas (LPG)/combustion, and tailpipe emission from motor vehicles, were categorized in Cluster 1. Laboratory studies (George et al., 2017, 2015) also found that the cold start driving phase and cold ambient temperature increased VOC emissions up to several orders of magnitude, compared to emissions during other vehicle operation phases and warmer temperature testing, respectively. The 2,2-dimethylbutane, 2-methylpentane, 3-methylpentane, methylcyclopentane, and isoprene, were categorized in Cluster 2. Chang et al. (2006) noted

that 2,2-dimethylbutane, 2-methylpentane, 3-methylpentane, and methylcyclopentane showed good correlations with methyl *tert*-butyl ether (MTBE, a maker specific to gasoline-related sources, can be present in both evaporative and tailpipe emissions from gasoline-powered vehicles) (Zhang et al., 2013b; Poulopoulos and Philippopoulos, 2000) in traffic environments. Thus, the gasoline-related VOC species in Cluster 2 might be associated with evaporative emissions from gasoline vehicles. As expected, isoprene, which was transported to the monitoring site from emissions of different plant species in surrounding areas, exhibited very high temperature dependence (Steiner et al., 2010; Piero et al., 2004). Therefore, Cluster 2 was associated with both the evaporative emissions from motor vehicles and with biogenic emissions. For ethylene, propylene, and TEX (toluene, ethylbenzene, *m*, *p*-xylene, and *o*-xylene), key markers for emissions from anthropogenic sources (e.g., solvent use, industrial process, and petrochemical industry), were categorized into Cluster 3. However, the concentrations of VOC species in Cluster 3 showed a signal peak tendency with the maximum appearing when temperatures were in the most comfortable temperature range (i.e., 18–25°C) for the human body. The results implied that some anthropogenic activities varied with temperature, and that people were most active at the most comfortable temperatures (i.e., neither too hot nor too cold). Thus, real-world VOCs are influenced directly and indirectly by temperature, since some anthropogenic activities are also largely influenced by temperature.

Fig. 2c shows the relationships between the VOCs by different criteria (the concentrations by volume and carbon atoms, the MIR-weighted concentrations, and the Propy-Equiv concentrations) and ambient temperature. The responses of the VOCs by volume and carbon atoms to temperature exhibited V-shape patterns, and the inflection points occurred when temperatures were around 15–25°C. However, the MIR-weighted and Propy-Equiv VOC concentrations generally increased with increase of the temperature. Thus, the VOCs by volume and by carbon atoms were mostly Cluster 1 and Cluster 2 when temperatures were lower and higher than 15–25°C, respectively. Additionally, the VOC reactivity was generally dominated by the cluster 2 since the pattern of temperature dependence of VOC reactivity (Fig. 2a) was similar to that of Cluster 2 (Fig. 2c), which might be associated with both the evaporative emissions from motor vehicles and from biogenic emissions. The results implied that temperature can be used as a proxy for VOC reactivity, which is consistent with Pusede and Cohen (2012). Furthermore, O₃ episodes frequently occurred during hot days on the NCP and are likely associated with the high temperature

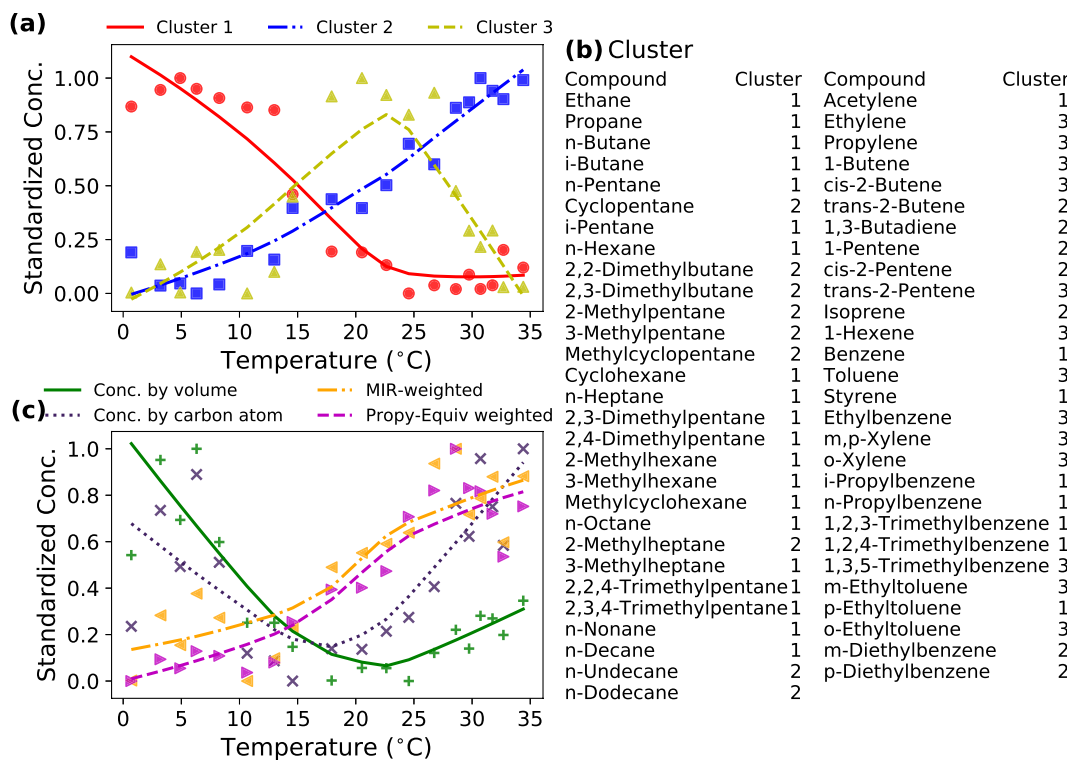


Fig. 2. The cluster analysis of (a) responses of the VOC species to temperature, (b) the VOC species that appeared in each cluster, and (c) the relationships between VOC concentrations by different criteria (the concentrations by volume and carbon atoms, the MIR-weighted concentrations, and the Propy-Equiv concentrations) and ambient temperature. The scatters are fitted by locally weighted polynomial regression (LOWESS).

dependence of VOC reactivity.

The ambient ratio of two VOC species is often used either to explore the characteristics of VOC compositions in emission sources (Ait-Helal et al., 2015; Steinbacher et al., 2005; Hedberg et al., 2002) or as a chemical clock for the determination of the photochemical age of air masses (Du et al., 2018; Nelson and Quigley, 1983). Among the VOC species, toluene and benzene, ethylbenzene and *m, p*-xylene, and *i*-butane and n-butane; are often found to be well correlated in ambient measurements (Zheng et al., 2018; Liu et al., 2008; Khoder, 2007). In addition, the ratio of propane to ethylene can be applied to distinguish natural gas sources from vehicle emissions (Gilman et al., 2013). In our case, the significant positive correlations (Fig. S7) between the mixing ratios of toluene and benzene ($R^2 = 0.56, p < 0.01$), ethylbenzene and *m, p*-xylene ($R^2 = 0.91, p < 0.01$), *i*-butane and n-butane ($R^2 = 0.94, p < 0.01$), and propane and ethylene ($R^2 = 0.38, p < 0.01$); were also observed at the site.

Fig. 3 illustrates the relationships between the diagnostic ratios and temperatures. The average toluene/benzene, ethylbenzene/*m, p*-xylene, *i*-butane/n-butane, and propane/ethylene ratios were 1.3 (95%CI: 0.4, 3.4), 1.2 (95%CI: 0.6, 3.3), 1.9 (95%CI: 0.2, 3.1), and 9.9 (95%CI: 0.9, 30.9), respectively. According to the source profiles in China (Zhang et al., 2016; Liu et al., 2008), the toluene/benzene ratios were < 1 for biomass/biofuel/coal burning, 1–10 for vehicle emissions, and > 1 for industrial processes and solvent use. In our case, the average ratio of toluene/benzene was 1.3 (95%CI: 0.4, 3.4), around one, which made it difficult to distinguish different emission sources because the value of toluene/benzene overlapped those of other sources (Zhang et al., 2016). The ratio of (ethylbenzene/*m, p*-xylene and *i*-butane/n-butane) was more than (twice and three times) the value of that from primary vehicle emissions (0.43 ± 0.16 for ethylbenzene/*m, p*-xylene, 0.63 ± 0.28 for *i*-butane/n-butane) in China (Song et al., 2018). This suggested that the ethylbenzene/*m, p*-xylene and *i*-butane/n-butane ratios were the combined results of emissions from both vehicular and non-vehicular sources.

The toluene/benzene, ethylbenzene/*m, p*-xylene, and *i*-butane/n-butane ratios were generally at low levels at low temperatures. However, the propane/ethylene ratio at low temperatures exhibited unexpectedly high values. The highest propane/ethylene ratio ($T = 7.5 \sim 12.0$ °C, as shown in Fig. S7 and Table S4) was 20.8 (95%CI: 12.7, 49.3) ($p < 0.01$), which is more than twice the value derived from overall regression (8.60 (95%CI: 8.31, 8.90), $p < 0.01$). This might be attributed to domestic heating-related emissions from NG/LPG sources at low temperatures. Zheng et al. (2018) reported that the propane/ethylene ratio was approximately 16:1 at an oil and natural gas station in northwest China, which is much higher than that in urban areas, such as 8.6:1 in Langfang in 2016 (this study), 1.5:1 in Guangzhou in 2011 (Zou et al., 2015), and 1:1 in Tianjin in 2015 (Liu et al., 2016). Elevated propane/ethylene in Langfang in 2016 was observed as compared to that in Tianjin in 2015 (Liu et al., 2016) because of the full implementation of the ‘coal-to-natural gas’ project in key cities in NCP in 2016.

3.3. Source apportionment of VOCs

For a meticulous understanding of the temperature dependence of VOCs, qualitative research is not enough via the concentrations and characteristic ratios. Source apportionment of ambient VOCs was carried out to quantitatively analyze the temperature dependence of source-specific VOCs. Six factors were resolved through application of the PMF model. Fig. 4 presents the source profiles of VOCs as modeled by PMF, and the corresponding hourly concentrations for each identified source.

High loadings of aromatic species (toluene, ethylbenzene, 1,2,4-Trimethylbenzene, *o*-xylene, and *m, p*-xylene) were found in Factor 1 (Fig. 4), and the average fractions of toluene, ethylbenzene, 1,2,4-Tri-methylbenzene, *o*-xylene, and *m, p*-xylene were 33.6%, 76.1%, 85.1%, 93.9%, and 90.2%, respectively. This factor was considered to be related to solvent use because of TEXs (including toluene, ethylbenzene,

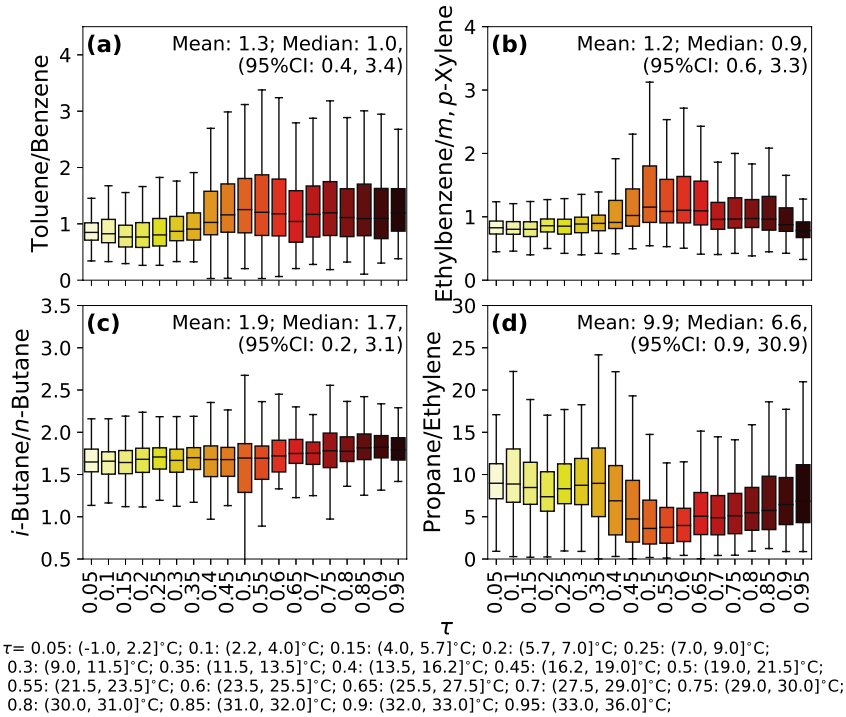


Fig. 3. Relationships between the diagnostic ratios (a: toluene/benzene, b: ethylbenzene/ *m, p*-Xylene, c: *i*-butane/n-butane, and d: propane/ethylene) and temperatures. Temperature sections (τ , cut by 19 quantiles, from 0.05 to 0.95 for every 0.05 quantile) are denoted below the figure.

o-xylene, and *m, p*-xylene) are major constituents of solvents (Yuan et al., 2010, 2009; Seila et al., 2001). Solvent use is generally associated with paint application, printing processes, dry cleaning, solvent evaporation from household products, and other industrial process. Yuan et al. (2010) noted that toluene and C8 aromatics were the most abundant species emitted from solvent use. It was estimated that VOC emissions from solvent use in China were about 2.7 Tg in 2000 (Klimont et al., 2002), and 4.3 Tg in 2013 (Wu and Xie, 2017); thus accounting for 17.4% and 14.4% of anthropogenic VOC emissions, respectively. According to the emission inventory for VOCs (Table S5), the annual amount of VOC emissions from solvent use was about 6854 t, including industrial painting (207 t), automobile service (941 t), pesticide use (1456 t), architectural coatings (1371 t), other non-industrial solvent use (2879 t).

Factor 2 was identified as petrochemical industry because of the high fractions of ethylene (97.0%), propene (45.1%), and n-hexane (44.2%). Moreover, high fractions of benzene (25.8%), ethylbenzene (12.4%), and toluene (37.4%) were also found in Factor 2. Jobson et al. (2005) reported that ethylene, propene, and n-hexane were source signatures of petrochemical industry emissions. The propene, n-hexane, benzene, and toluene were also abundant in chemical profiles measured in a petroleum refinery in Beijing (Wei et al., 2014). In Langfang, the ambient VOCs from petrochemical industry emissions might have originated from the chemical industrial district in Tianjin (Liu et al., 2016; Han et al., 2015), one of the largest industrial cities in the NCP. Thus, Factor 2 was identified as petrochemical industry.

Factor 3 shows the predominance of n-pentane (50.1%) and n-hexane (49.2%) in the source profile. The pentanes are some of the primary blowing agents used in the production of polystyrene foam and other foams, whereas n-hexane is an ingredient of special glues that are used in the roofing, shoe, and leather industries. It (n-hexane) is also used in binding books, working leather, shaping pills and tablets, canning, manufacturing tires, and making baseballs. Meanwhile, Factor 3 shows a linear relationship (Pearson's $r = 0.6$, $p < 0.01$) with ambient temperature. Based on the VOC emission inventory for VOCs (Table S5), the industrial process sources were mainly metal manufacturing,

petrochemical industry, coking industry, cements, plate glass, and others. However, TEXs (source signals for solvent use), and ethylene and propene (source signals for petrochemical industry), were not abundant in Factor 3. Thus, Factor 3 was identified as other industry processes, excluding solvent use and the petrochemical industry.

Factor 4 is distinguished by a significant amount of *i*-butane (96.8%), n-butane (87.3%), *i*-pentane (98.4%), n-pentane (49.9%), 3-methylpentane (99.9%), propane (44.5%), and benzene (34.3%), which are typical tracers of vehicle emissions. Factor 4 also shows a linear relationship (Pearson's $r = 0.6$, $p < 0.01$) with ambient NO₂, mainly originated from vehicle emissions in urban areas. In general, *i*-pentane, toluene, ethylene, *i*-butane, and n-butane are the species frequently observed as most abundant in vehicle emissions (including tailpipe and evaporative emissions) from tunnel studies (Cui et al., 2018; Zhang et al., 2018a, b; Ho et al., 2009). The *i*-pentane, n-pentane, and toluene are primary indicators of gasoline evaporation (Yue et al., 2017; Liu et al., 2008; Tsai et al., 2006; Hwa et al., 2002). Therefore, Factor 4 was identified as vehicle emission, including both tailpipe and evaporative emissions. According to the emission inventory for VOCs (Table S5), the annual amount of VOC emissions from vehicles is about 19,770 t, including gasoline vehicles (11,740 t), diesel vehicles (5239 t), alternative-fuel vehicles (913 t), and non-road vehicles (1878 t).

Factor 5 is rich in acetylene (99.9%), ethane (72.3%), propane (43.7%), and benzene (27.0%) in the source profile. Acetylene is a key marker for combustion sources (Zheng et al., 2018; Wang et al., 2014, 2010; Watson et al., 2001), while ethane and propane are the most abundant species in NG/LPG (Zheng et al., 2018; An et al., 2014; McCarthy et al., 2013; Ling et al., 2011). The VOC concentrations attributed to Factor 5 were larger at wintertime because more fuel was burned for domestic heating in the NCP. Factor 5 also correlated well (Pearson's $r = 0.6$, $p < 0.01$) with CO, a key tracer for incomplete combustion processes, further indicating that Factor 5 is associated with heating-related sources. The full implementation of changing fuel from coal to natural gas in key cities on the NCP (Song et al., 2017b; Liu et al., 2016) made NG/LPG became a key contributor to ambient VOCs during heating periods. Thus, Factor 5 was identified as NG/LPG/

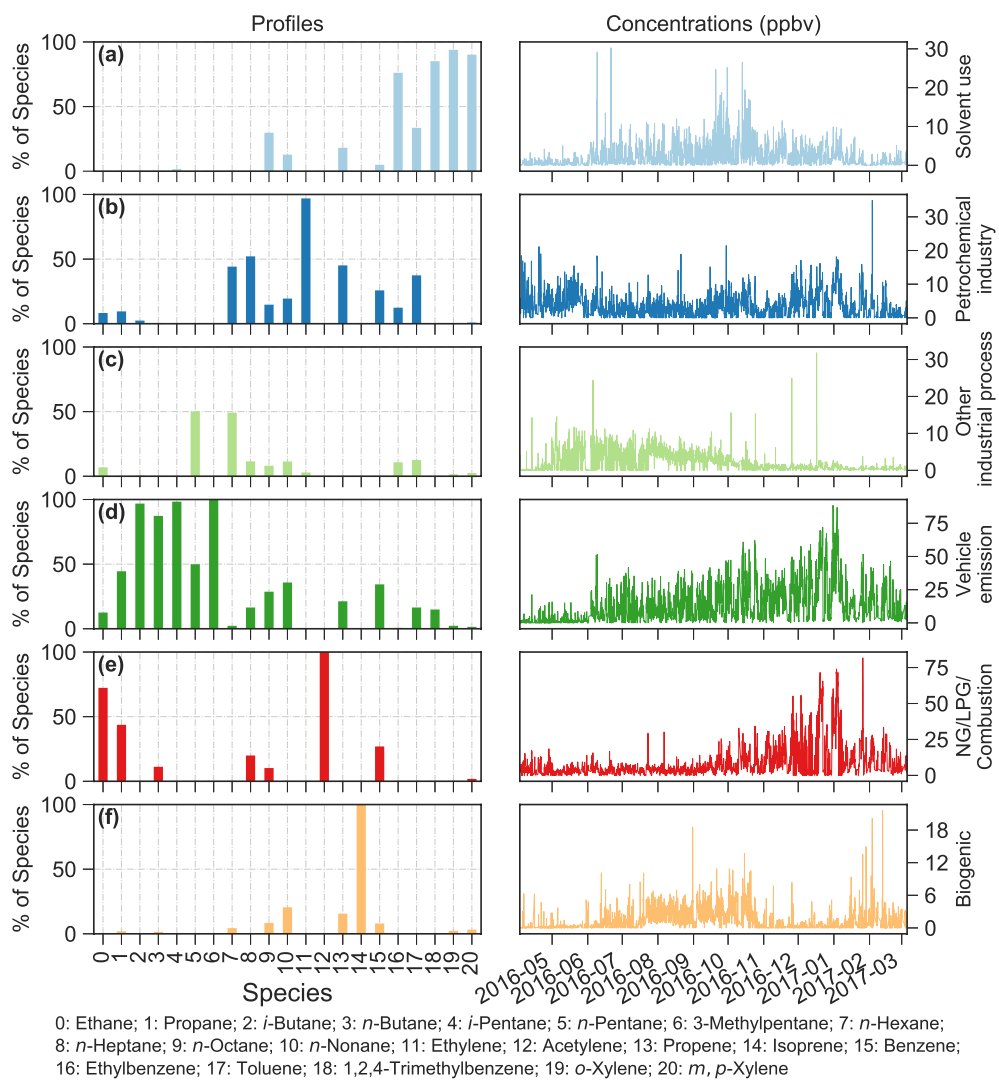


Fig. 4. Source profiles (% of species) of six factors resolved with PMF model including (a) solvent use, (b) petrochemical industry, (c) other industrial process, (d) vehicle emission, (e) NG/LPG/Combustion, and (f) biogenic and their corresponding hourly source concentrations.

Combustion in this study.

Factor 6 is distinguished by a significant presence of isoprene, the most abundant compound from biogenic emissions, especially from broad-leaved trees (Yuan et al., 2009; Kesselmeier and Staudt, 1999). Isoprene emissions account for about half of the total BVOC emissions, which play a critical role in biosphere-atmosphere interactions and are key factors of the physical and chemical properties of the atmosphere and climate. Isoprene also forms a higher quantity of OFP because of its higher reactivity, compared to other BVOCs. The VOC concentrations attributed to Factor 6 were higher in summer because of higher temperature and solar radiation, compared to other seasons.

Overall, these resolved factors were identified as Factor 1: solvent use, Factor 2: petrochemical industry, Factor 3: other industry processes, Factor 4: vehicle emission, Factor 5: NG/LPG/Combustion, and Factor 6: biogenic emission. The resolved source profiles (% of species) and hourly contributions (ppbv) for each factor are shown in Fig. 4. Approximately 94% of the ambient VOCs in Langfang were explained using the PMF (Fig. S8h). Moreover, for the individual VOCs species, the PMF model also reproduced the predicted values well (Figs. S8a–g). Therefore, we considered that the ambient VOCs concentrations measured at the monitoring site could be adequately resolved using these six factors in the PMF model.

Fig. 5 (the data are listed in Table S6) shows the variation in monthly and seasonally averaged contributions of the six identified

VOC sources. Each resolved source exhibited obvious temporal variation because of anthropogenic emission patterns, meteorological conditions, and photochemical reactions. Vehicle emissions made the largest contribution to the ambient VOCs throughout the year, with an average value of 44.8% over the entire year and ranging from 42.2% in the summer to 47.6% in the winter. Based on the emission inventory in Langfang (Table S5), gasoline vehicles, diesel vehicles, alternative-fuel vehicles, and non-road vehicles contributed (respectively) 59.4%, 26.5%, 4.6%, and 9.5% to VOC emissions from vehicles. Thus, the annual contributions of gasoline vehicles, diesel vehicles, alternative-fuel vehicles, and non-road vehicles to the ambient VOCs were estimated to be 26.6%, 11.9%, 2.1%, and 4.2%, respectively.

Previous studies revealed that vehicle emissions contributed the most to ambient VOCs in the cities neighboring Langfang, such as Beijing (contribution of 38.5–62%) (Gao et al., 2018; Wang et al., 2016; Yuan et al., 2009), and Tianjin (contribution of 37.2–60%) (Liu et al., 2016; Han et al., 2015). By the end of 2017, vehicle populations in Beijing and Tianjin ranked 1st (5.6 million) and 8th (2.9 million) among Chinese cities, respectively. Vehicle emissions, including tailpipe and evaporative emissions, appear to be major sources of ambient VOCs in urban areas on the NCP. The NG/LPG/Combustion sources were the second highest contributors (a contribution of 24.9%) to ambient VOCs in Langfang because of full implementation of the ‘coal-to-natural gas’ project in key cities of the NCP (Song et al., 2017b). The

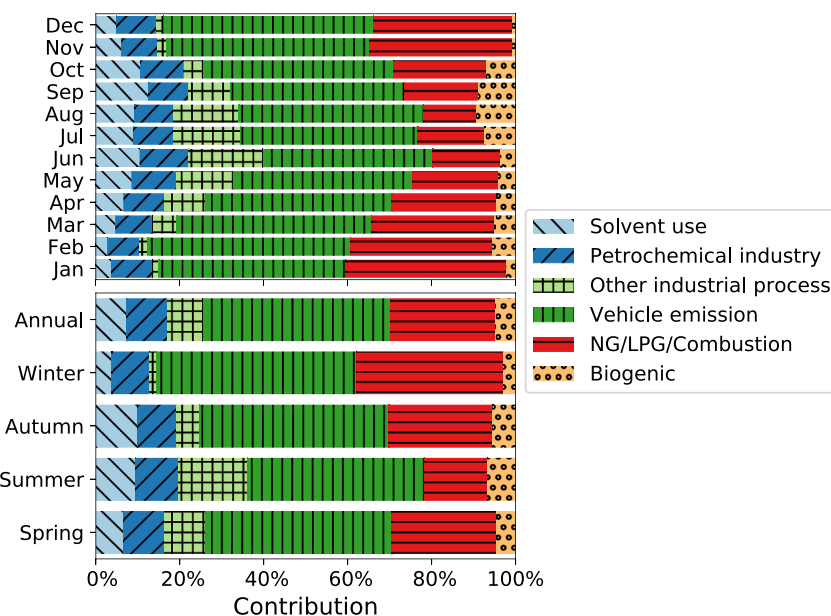


Fig. 5. Relative contributions of each source (solvent use, petrochemical industry, other industrial process, vehicle emission, NG/LPG/Combustion, and biogenic) to the ambient VOCs for each month (from Jan to Dec), each season (from spring to winter), and the entire year.

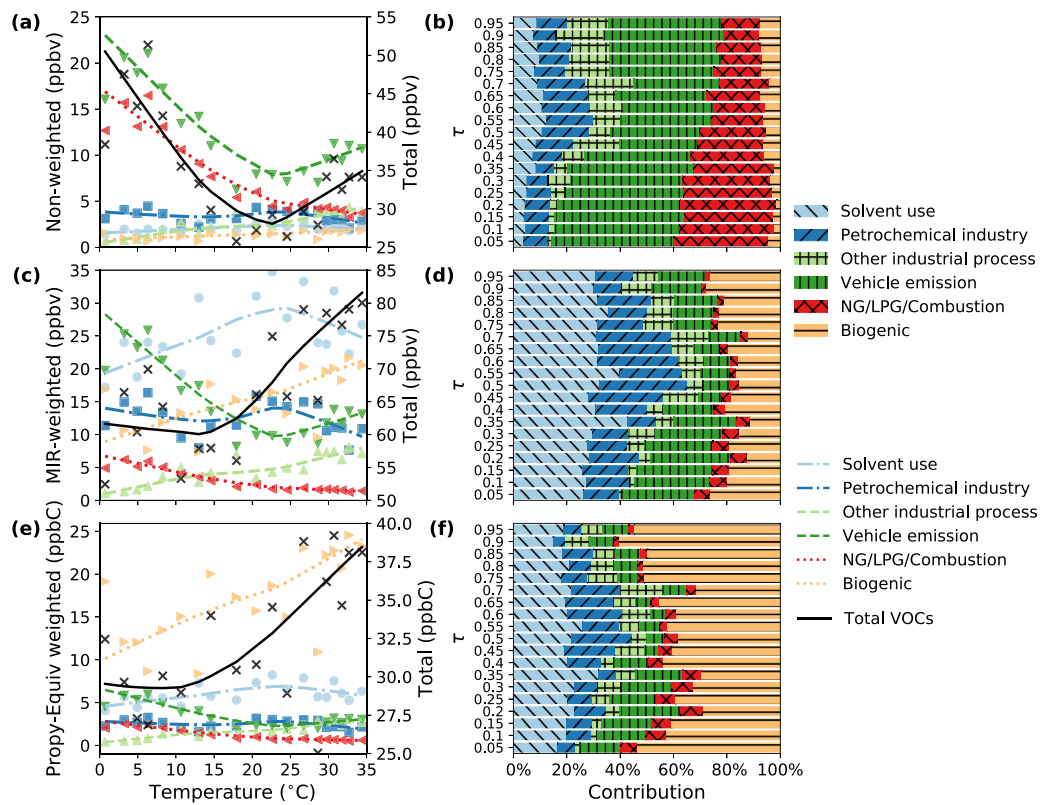
contribution of NG/LPG/Combustion sources exhibited temporal variations, being highest in winter (35.1%) and lowest in summer (15%), further verifying that these sources are associated with domestic heating. Thus, vehicle emission (gasoline vehicles: 26.6%, diesel vehicles: 11.9%, alternative-fuel vehicles: 2.1%, and non-road vehicles: 4.2%) and NG/LPG/Combustion (24.9%) were the major sources, contributing a total of 69.7% (ranging from 57.2% in summer to 82.7% in winter) of ambient VOCs in Langfang. This was followed by the petrochemical industry (9.6%), other industrial process (8.4%), solvent use (7.4%), and biogenic emission (4.9%). It is likely that gasoline vehicles are the primary sources of VOC emissions in Langfang during the study period.

3.4. Temperature dependence of source-specific VOCs

The temporal variations of contributions of the identified sources to ambient VOCs could be mainly attributed to temperature-dependent VOC emissions. Here, we present the temperature-dependent VOC concentrations and contributions (including non-weighted, MIR-weighted, and Propy-Equiv weighted concentrations) of each identified source in Fig. 6. The V-shaped pattern of the temperature-dependent VOCs from vehicle emissions was observed, which might be attributable to comprehensive effects of cold engine starts (tailpipe emission) and gasoline evaporation. By comparison with 25 °C, the VOC emissions from vehicles were approximately seven times greater at zero °C (i.e., 0–25 °C: 28% °C⁻¹), and 50.4% greater at 35 °C (i.e., 25–35 °C: 5% °C⁻¹). Laboratory study also suggested that the cold start driving phase and cold ambient temperature increased VOC emissions up to several orders of magnitude compared to emissions during other vehicle operation phases and warm ambient temperature testing (George et al., 2015). In addition, a similar pattern was also observed for NO_x emissions. Singh and Sloan (2006) noted that by comparison with 20 °C, emission rates were higher by approximately 42% at -10 °C (i.e., -10–20 °C: ~1.5% °C⁻¹) because of the cold engine starts and 16% at 35 °C (i.e., 20–35 °C: ~1% °C⁻¹) because of air-conditioning and the cold engine starts. A previous tunnel study (Song et al., 2018) reported that vehicular NO_x and VOCs could be co-emitted with a proper emission ratio, further indicating the V-shape pattern of temperature-dependent VOCs and NO_x from vehicle emissions. Besides, by comparison with 25 °C, the VOC emissions from NG/LPG/Combustion were

approximately 3.8 times greater at zero °C (i.e., 0–25 °C: 15.3% °C⁻¹), and were unchanged when ambient temperature was higher than 25 °C. The temperature-dependent VOC emissions from NG/LPG/Combustion were fairly reasonable because this factor was associated with domestic heating in the NCP. The VOCs emitted from other sources generally showed linear relationships with ambient temperature. By comparison with 0 °C, the VOCs from solvent use, other industrial process, and biogenic emissions increased by approximately ~1.0% °C⁻¹ (the linear regression: $y = 0.02x + 1.7$, $R^2 = 0.2$), ~14.5% °C⁻¹ (the linear regression: $y = 0.1x + 0.7$, $R^2 = 0.8$), ~2.6% °C⁻¹ (the linear regression: $y = 0.02x + 0.9$, $R^2 = 0.4$), respectively. Since vehicle emissions were the predominant portion of ambient VOCs throughout the entire range of temperatures ($\tau = 0.05 \sim 0.95$), the patterns of temperature-dependent VOC emissions were likely to be similar with those from vehicle emissions (i.e., the V-shaped pattern). By comparison with 25 °C, the total VOC emissions are higher by approximately 96% at 0 °C (i.e., 0–25 °C: ~3.8% °C⁻¹) and 31.3% at 31.3 °C (i.e., 20–35 °C: ~3.1% °C⁻¹). In summary, the major sources of ambient non-weighted VOCs at low temperatures ($\tau = 0.05 \sim 0.5$, i.e., -1–21.5 °C) were as follows: vehicle emission (42.2 ± 6.5%), NG/LPG/Combustion (31.6 ± 4.3%), petrochemical industry (10.6 ± 3.3%), solvent use (6.1 ± 2.3%), other industrial process (5.9 ± 4.8%), and biogenic emission (3.6 ± 1.7%). The source that contributed the most to ambient non-weighted VOCs at high temperatures ($\tau = 0.5 \sim 0.95$, i.e., 21.5–36.0 °C) was vehicle emission (38.1 ± 4.7%), followed by NG/LPG/Combustion (17.3 ± 2.4%), other industrial process (14.4 ± 3.0%), petrochemical industry (14.1 ± 3.7%), solvent use (9.5 ± 1.6%), and biogenic emission (6.6 ± 1.2%).

The temperature-dependent VOC concentrations, as weighted by the MIR (Fig. 6c and d) and Propy-Equiv (Fig. 6e and f), were also characterized. Vehicle emission and solvent use basically dominated the MIR-weighted VOC concentrations when the ambient temperature was below 15°C. At high ambient temperature ($T > 25^\circ\text{C}$), the dominant sources of MIR-weighted concentrations were solvent use (31.8 ± 1.8%) and biogenic emissions (21.8 ± 5.1%). The MIR-weighted and Propy-Equiv weighted VOC concentrations for biogenic emissions increased rapidly with the ambient temperature, suggesting that, especially at high temperatures, biogenic emissions also need to be considered with respect to the control of O₃. Although solvent use and biogenic emissions contributed only 7.4% and 4.9% to the VOCs by



$$\tau = 0.05: (-1.0, 2.2)^{\circ}\text{C}; 0.1: (2.2, 4.0)^{\circ}\text{C}; 0.15: (4.0, 5.7)^{\circ}\text{C}; 0.2: (5.7, 7.0)^{\circ}\text{C}; 0.25: (7.0, 9.0)^{\circ}\text{C}; 0.3: (9.0, 11.5)^{\circ}\text{C}; 0.35: (11.5, 13.5)^{\circ}\text{C}; 0.4: (13.5, 16.2)^{\circ}\text{C}; 0.45: (16.2, 19.0)^{\circ}\text{C}; 0.5: (19.0, 21.5)^{\circ}\text{C}; 0.55: (21.5, 23.5)^{\circ}\text{C}; 0.6: (23.5, 25.5)^{\circ}\text{C}; 0.65: (25.5, 27.5)^{\circ}\text{C}; 0.7: (27.5, 29.0)^{\circ}\text{C}; 0.75: (29.0, 30.0)^{\circ}\text{C}; 0.8: (30.0, 31.0)^{\circ}\text{C}; 0.85: (31.0, 32.0)^{\circ}\text{C}; 0.9: (32.0, 33.0)^{\circ}\text{C}; 0.95: (33.0, 36.0)^{\circ}\text{C};$$

Fig. 6. Temperature-dependent VOC concentrations (left panel, a: non-weighted, c: maximum-incremental-reactivity (MIR) weighted, e: propylene-equivalent (Propy-Equiv) weighted) and contributions (right panel, b: non-weighted, d: MIR-weighted, f: Propy-Equiv weighted) of each identified source (solvent use, petrochemical industry, other industrial process, vehicle emission, NG/LPG/Combustion, and biogenic). The scatters in the left panel of the figure are fitted by locally weighted polynomial regression (LOWESS). The temperature sections (τ , cut by 19 quantiles, from 0.05 to 0.95 for every 0.05 quantile) are denoted below the figure.

volume, they ranked first ($31.2 \pm 4.3\%$) and third ($19.0 \pm 4.8\%$), respectively, in terms of maximum-incremental reactivity; and ranked second ($20.7 \pm 3.6\%$) and first ($42.8 \pm 8.9\%$), respectively, in terms of OH reactivity. On the other hand, vehicle emissions, which accounted for almost half (44.8%) of the VOCs by volume, contributed only $18.4 \pm 7.2\%$ (ranked forth) to the MIR-weighted VOCs and $11.9 \pm 5.6\%$ (ranked forth) to the Propy-Equiv weighted VOCs. This may be a result of alkanes with low reactivity dominating vehicle emissions (Song et al., 2018; Cui et al., 2018; Zhang et al., 2018b). By comparison with 25°C , the MIR-weighted VOCs from vehicles were approximately 2.6 times greater at 0°C (i.e., $0 \sim 25^{\circ}\text{C}$: $10.4^{\circ}\text{C}^{-1}$), and 57.5% greater at 35°C (i.e., $25 \sim 35^{\circ}\text{C}$: 5.8°C^{-1}). Laboratory study also suggested that the estimated OFPs were 7–21 times greater for the cold starts during cold temperature tests than during comparable warm temperature tests (George et al., 2015).

Despite that the patterns of temperature-dependent VOC emissions (Fig. 6a), was likely to be the V-shape pattern, the temperature dependence of the MIR-weighted (Fig. 6c) and Propy-Equiv weighted (Fig. 6d) VOC concentrations were in exponential or polynomial forms. Moreover, temperature dependence of the MIR-weighted and Propy-Equiv weighted VOCs might be more sensitive and underestimated because of the effects of OH removal. Overall, solvent use was the greatest contributor ($31.2 \pm 4.3\%$) to the MIR-weighted VOCs throughout the entire range of temperatures, and was followed by the petrochemical industry ($19.6 \pm 6.9\%$), biogenic emission ($19.0 \pm 4.8\%$), vehicle emission ($18.4 \pm 7.2\%$), other industrial process ($7.7 \pm 3.5\%$), and NG/LPG/Combustion ($4.1 \pm 1.8\%$). Biogenic emission was the largest contributor ($42.8 \pm 8.9\%$) to the Propy-Equiv weighted VOCs for the entire range of temperatures, and was

followed by solvent use ($20.7 \pm 3.6\%$), the petrochemical industry ($12.1 \pm 5.3\%$), vehicle emission ($11.9 \pm 5.6\%$), other industrial process ($7.5 \pm 3.6\%$), and NG/LPG/Combustion ($5.0 \pm 2.3\%$). Considering the VOC reactivity, control of solvent use could be the best priority for emission reductions for O_3 control in the NCP during hot days.

3.5. Potential source-areas of VOCs

The local air quality in the NCP is profoundly influenced by regional sources and transport of air pollutants (Liu et al., 2016; Zhang et al., 2013a). Backward trajectory analysis was used to reveal the transport pathways of the air masses. During the study period, the trajectories were clustered into four groups (Fig. S1) (1), (2), (3), and (4). Trajectory cluster (1), accounting for 33.8% of the total, originated from Hengshui city, and passed through south of Hebei province before arriving at Langfang. Trajectory cluster (2), accounting for 25.0% of the total trajectories, originated from Tangshan city, and passed through Tianjin before arriving at Langfang. Trajectory (1) and (2), together accounting for 58.8% of the total trajectories, reflected the features of small-scale, short-distance air mass transport (Fig. S1). Trajectory (3) and (4), accounted for 24.9% and 16.3% of the total trajectories, respectively, that originated from Mongolia and Inner Mongolia and passed through Hebei province and Beijing, showed the features of large-scale, long-distance air mass transport. Annually, the trajectory clusters were dominated by short-distance air mass transport (i.e., trajectory cluster (1) and (2)).

The PSCF model was used to identify possible geographic origins of the six identified VOC sources (Fig. 7). As shown in Fig. 7a, the

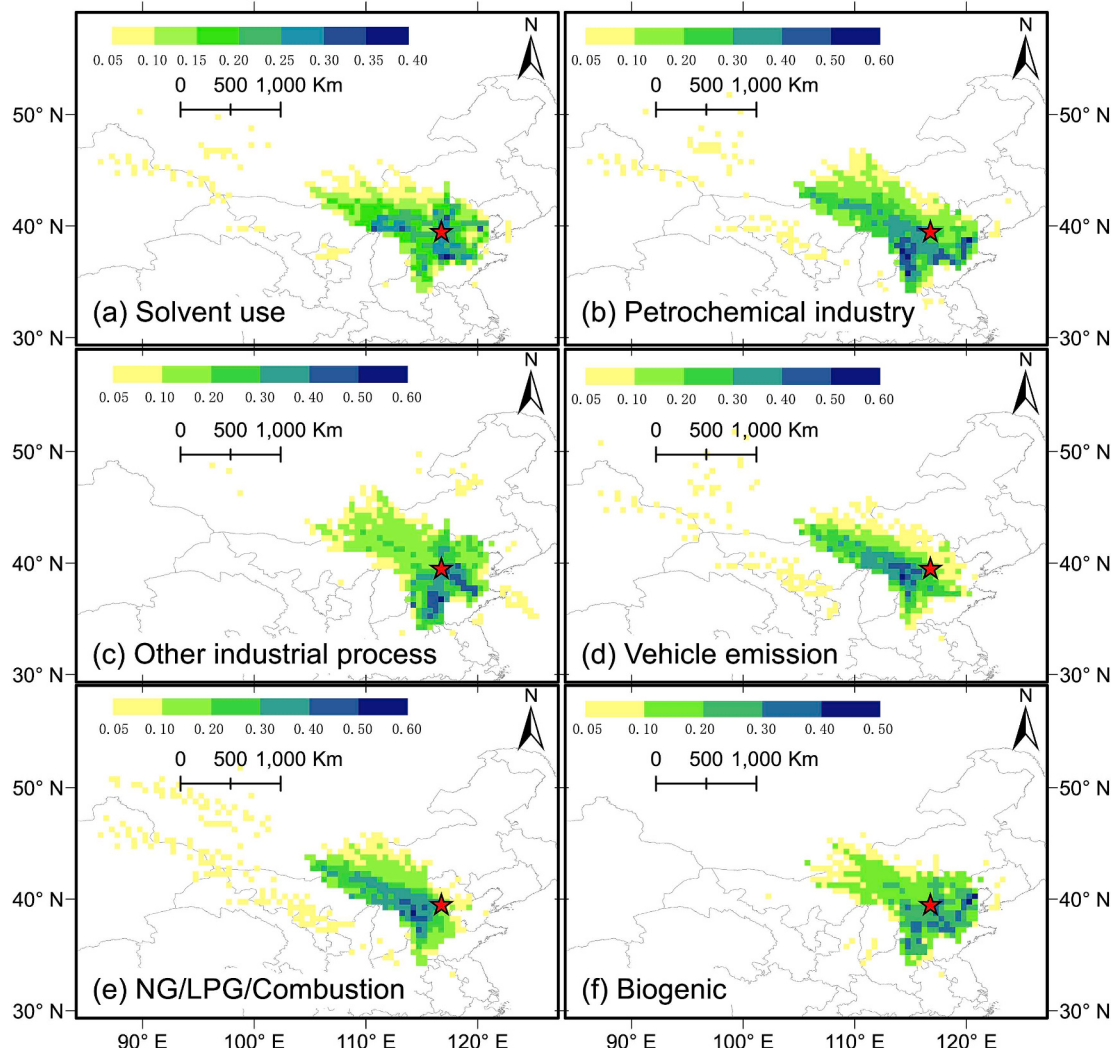


Fig. 7. WPSCF maps of (a) solvent use, (b) petrochemical industry, (c) other industrial process, (d) vehicle emission, (e) NG/LPG/Combustion, and (f) biogenic emissions for the entire year in Langfang.

geographic origins of solvent use were almost evenly distributed in the NCP. Solvents, the greatest contributors to MIR-weighted VOCs and second contributors to Propy-Equiv VOCs, were widely used in urban areas for paint application, printing processes, dry cleaning, and so on. Regarding the petrochemical industry (Fig. 7b) and other industry processes (Fig. 7c), our PSCF results showed that short-distance air mass originated from the south of Hebei Province and the north of Shandong Province were the major pathways of transport. The south of Hebei Province and the north of Shandong Province were the hotspots of air pollution in China according to data from the air quality monitoring stations (Song et al., 2017a, b). Thus, industrial emissions, including the petrochemical industry and other industry process, might contribute the most to air pollution in these most polluted regions. For vehicle emissions (Fig. 7d) and NG/LPG/combustion (Fig. 7e), long-distance air transport originating from Mongolia and Inner Mongolia also contributed to the VOC concentrations in Langfang, apart from the short-distance transport from the neighboring megacities (e.g., Beijing and Tianjin). The results suggested that alkanes-dominated VOC sources (e.g., vehicle emission, NG/LPG) could experience long-distance air transport because of their relatively long atmospheric lifetime. Similar potential geographic sources of vehicle emissions (Fig. 7d) and NG/LPG/combustion (Fig. 7e) were found in the NCP because these sources are associated with anthropogenic fossil fuel combustion. For biogenic emissions (Fig. 7f), high local contributions that originated in

cities in the NCP were observed from the PSCF results. The VOCs from biogenic emission are very unlikely experiencing long-distance air transport due to their high OH reactivities.

The VOC concentrations in Langfang in the NCP were less influenced by long-distance air masses originating from the southwest direction because of the Taihang Mountains. Overall, the local emissions in the NCP (south of Yanshan Mountains and east of Taihang Mountains) were the major sources of ambient VOCs in Langfang. Local emission controls for VOCs are beneficial for alleviating atmospheric secondary pollution because the potential source-areas of source-specific VOCs were mostly distributed within the geographically flat NCP.

4. Conclusions

Based on one year of observations of ambient VOCs in urban Langfang, the temperature dependence of VOCs and their potential sources were revealed. The VOC reactivity was mainly due to alkenes, though alkanes contributed the most to the VOCs both by volume and by carbon atoms. The patterns of temperature-dependent VOC species could be categorized into three clusters, indicating that the real-world VOCs were influenced directly and indirectly by temperature. Nevertheless, the VOC reactivities generally increased with increase of the temperature, suggesting that temperature could be used as a proxy for VOC reactivities.

On average, vehicle emissions (44.8%) contributed the most to ambient VOCs in Langfang, and were followed by NG/LPG/Combustion (24.9%), petrochemical industry (9.6%), other industrial process (8.4%), solvent use (7.4%), and biogenic emissions (4.9%). Despite that solvent use and biogenic emissions contributed the least to the VOCs by volume, they were the greatest contributors to VOC reactivity. Consequently, control of solvent use could be the best priority for emission reduction for O₃ control in the NCP during hot days.

Unexpectedly high propane/ethylene ratios were observed at low temperatures, which might be associated with domestic heating-related emissions from NG/LPG sources because their contributions generally increased with decrease of the temperature. Since vehicle emissions dominated ambient VOCs throughout the entire range of temperatures, the pattern of temperature-dependent VOC emissions was likely to be similar with that of vehicle emissions (i.e., the V-shaped pattern), which was mainly associated with comprehensive effects of cold engine starts and evaporative emissions. Local emission controls for VOCs were beneficial for alleviating atmospheric secondary pollution because the potential source-areas of source-specific VOCs were mostly distributed within the geographically flat NCP. However, alkanes-dominated VOC sources (e.g., vehicle emission, NG/LPG) could experience long-distance transport because of their relatively long atmospheric lifetime.

The chemical loss of VOCs and its impact on the temperature-dependent VOCs needs to be investigated in the future. These results highlight that the temperature dependence of VOCs varies with different emission sources, and this is of great value in understanding the linkage between meteorology and air quality.

Acknowledgements

This work was funded by the National Key Research and Development Program of China (2017YFC0212104).

Appendix A. Supplementary data

Supplementary data to this article can be found online at <https://doi.org/10.1016/j.atmosenv.2019.03.030>.

References

- Abel, D., Holloway, T., Kladar, R.M., Meier, P., Ahl, D., Harkey, M., Patz, J., 2017. Response of power plant emissions to ambient temperature in the eastern United States. *Environ. Sci. Technol.* 51, 5838–5846. <https://doi.org/10.1021/acs.est.6b06201>.
- Alt-Helal, W., Beeldens, A., Boonen, E., Borbon, A., Borave, A., Cazaunau, M., Chen, H., Dale, V., Dupart, Y., Gaimoz, C., Gallus, M., George, C., Grand, N., Grosselin, B., Herrmann, H., Ifang, S., Kurtenbach, R., Maille, M., Marjanovic, I., Mellouki, A., Miet, K., Mothes, F., Poulain, L., Rabe, R., Zapf, P., Kleffmann, J., Doussin, J.F., 2015. On-road measurements of nmvoxs and nox determination of light-duty vehicles emission factors from tunnel studies in brussels city center. *Atmos. Environ.* 122, 799–807. <https://doi.org/10.1016/j.atmosenv.2015.09.066>.
- An, J., Zhu, B., Wang, H., Li, Y., Lin, X., Yang, H., 2014. Characteristics and source apportionment of vocs measured in an industrial area of nanjing, yangtze river delta, China. *Atmos. Environ.* 97, 206–214. <https://doi.org/10.1016/j.atmosenv.2014.08.021>.
- Atkinson, R., Arey, J., 2003. Atmospheric degradation of volatile organic compounds. *Chem. Rev.* 103, 4605–4638. <https://doi.org/10.1021/cr0206420>.
- Carter, W.P., 1994. Development of ozone reactivity scales for volatile organic compounds. *Air Waste* 44, 881–899. <https://doi.org/10.1080/1073161X.1994.10467290>.
- Chameides, W.L., Fehsenfeld, F., Rodgers, M.O., Cardelino, C., Martinez, J., Parrish, D., Lonneman, W., Lawson, D.R., Rasmussen, R.A., Zimmerman, P., Greenberg, J., Middleton, P., Wang, T., 1992. Ozone precursor relationships in the ambient atmosphere. *J. Geophys. Res.: Atmos.* 97, 6037–6055. <https://doi.org/10.1029/91JD03014>.
- Chang, C.C., Wang, J.L., Liu, S.C., Lung, S.C.C., 2006. Assessment of vehicular and non-vehicular contributions to hydrocarbons using exclusive vehicular indicators. *Atmos. Environ.* 40, 6349–6361. <https://doi.org/10.1016/j.atmosenv.2006.05.043>.
- Charrad, M., Ghazzali, N., Boiteau, V., Niknafs, A., 2014. Nbclust: an r package for determining the relevant number of clusters in a data set. *J. Statist. Software* 1–36. <https://doi.org/10.18637/jss.v061.i06>. Articles 61.
- Cui, L., Wang, X.L., Ho, K.F., Gao, Y., Liu, C., Ho, S.S.H., Li, H.W., Lee, S.C., Wang, X.M., Jiang, B.Q., Huang, Y., Chow, J.C., Watson, J.G., Chen, L.W., 2018. Decrease of voc emissions from vehicular emissions in Hong Kong from 2003 to 2015: results from a tunnel study. *Atmos. Environ.* 177, 64–74. <https://doi.org/10.1016/j.atmosenv.2018.01.020>.
- Deng, Y., Li, J., Li, Y., Wu, R., Xie, S., 2019. Characteristics of volatile organic compounds, no2, and effects on ozone formation at a site with high ozone level in chengdu. *J. Environ. Sci.* 75, 334–345. <https://doi.org/10.1016/j.jes.2018.05.004>.
- Dodge, M.C., 1984. Combined effects of organic reactivity and nmhc/nox ratio on photochemical oxidant formation modeling study. *Atmos. Environ.* 18, 1657–1665. [https://doi.org/10.1016/0004-6981\(84\)90388-3](https://doi.org/10.1016/0004-6981(84)90388-3).
- Du, Z., Hu, M., Peng, J., Zhang, W., Zheng, J., Gu, F., Qin, Y., Yang, Y., Li, M., Wu, Y., Shao, M., Shuai, S., 2018. Comparison of primary aerosol emission and secondary aerosol formation from gasoline direct injection and port fuel injection vehicles. *Atmos. Chem. Phys.* 18, 9011–9023. <https://doi.org/10.5194/acp-18-9011-2018>.
- Fu, T.M., Zheng, Y., Paultot, F., Mao, J., Yantosca, R., 2015. Positive but variable sensitivity of august surface ozone to large-scale warming in the southeast United States. *Nat. Clim. Change* 5, 454–458. <https://doi.org/10.1038/nclimate2567>.
- Gao, J., Zhang, J., Li, H., Li, L., Xu, L., Zhang, Y., Wang, Z., Wang, X., Zhang, W., Chen, Y., Cheng, X., Zhang, H., Peng, L., Chai, F., Wei, Y., 2018. Comparative study of volatile organic compounds in ambient air using observed mixing ratios and initial mixing ratios taking chemical loss into account a case study in a typical urban area in beijing. *Sci. Total Environ.* 628–629, 791–804. <https://doi.org/10.1016/j.scitotenv.2018.01.175>.
- Garzon, J.P., Huertas, J.I., Magaa, M., Huertas, M.E., Crdenas, B., Watanabe, T., Maeda, T., Wakamatsu, S., Blanco, S., 2015. Volatile organic compounds in the atmosphere of Mexico city. *Atmos. Environ.* 119, 415–429. <https://doi.org/10.1016/j.atmosenv.2015.08.014>.
- Gentner, D.R., Ford, T.B., Guha, A., Boulanger, K., Brioude, J., Angevine, W.M., de Gouw, J.A., Warneke, C., Gilman, J.B., Ryerson, T.B., Peischl, J., Meinardi, S., Blake, D.R., Atlas, E., Lonneman, W.A., Kleindienst, T.E., Beaver, M.R., Clair, J.M.S., Wennberg, P.O., VandenBoer, T.C., Markovic, M.Z., Murphy, J.G., Harley, R.A., Goldstein, A.H., 2014. Emissions of organic carbon and methane from petroleum and dairy operations in California's san joaquin valley. *Atmos. Chem. Phys.* 14, 4955–4978. <https://doi.org/10.5194/acp-14-4955-2014>.
- George, I., Hays, M., Snow, R., Faircloth, J., Long, T., Baldauf, R., 2017. Cold temperature effects on speciated voc emissions from modern gdi light-duty vehicles: preliminary results. In: Emissions Inventory Conference, Baltimore, MD. https://www.epa.gov/sites/production/files/2017-11/documents/cold_temperature.pdf.
- George, I.J., Hays, M.D., Herrington, J.S., Preston, W., Snow, R., Faircloth, J., George, B.J., Long, T., Baldauf, R.W., 2015. Effects of cold temperature and ethanol content on voc emissions from light-duty gasoline vehicles. *Environ. Sci. Technol.* 49, 13067–13074. <https://doi.org/10.1021/acs.est.5b04102>.
- Gilman, J., Lerner, B., Kuster, W., De Gouw, J., 2013. Source signature of volatile organic compounds from oil and natural gas operations in northeastern Colorado. *Environ. Sci. Technol.* 47, 1297–1305. <https://doi.org/10.1021/es304119a>.
- Guo, S., Hu, M., Zamora, M.L., Peng, J., Shang, D., Zheng, J., Du, Z., Wu, Z., Shao, M., Zeng, L., Molina, M.J., Zhang, R., 2014. Elucidating severe urban haze formation in China. *Proc. Natl. Acad. Sci. Unit. States Am.* 111, 17373–17378. <https://doi.org/10.1073/pnas.1419604111>.
- Han, M., Lu, X., Zhao, C., Ran, L., Han, S., 2015. Characterization and source apportionment of volatile organic compounds in urban and suburban tianjin, China. *Adv. Atmos. Sci.* 32, 439–444. <https://doi.org/10.1007/s00376-014-4077-4>.
- Hedberg, E., Kristensson, A., Ohlsson, M., Johansson, C., ke Johansson, P., Swietlicki, E., Vesely, V., Wideqvist, V., Westerholm, R., 2002. Chemical and physical characterization of emissions from birch wood combustion in a wood stove. *Atmos. Environ.* 36, 4823–4837. [https://doi.org/10.1016/S1352-2310\(02\)00417-X](https://doi.org/10.1016/S1352-2310(02)00417-X).
- Ho, K., Lee, S.C., Ho, W.K., Blake, D.R., Cheng, Y., Li, Y.S., Ho, S.S.H., Fung, K., Louie, P.K.K., Park, D., 2009. Vehicular emission of volatile organic compounds (vocs) from a tunnel study in Hong Kong. *Atmos. Chem. Phys.* 9, 7491–7504. <https://doi.org/10.5194/acp-9-7491-2009>.
- Hui, L., Liu, X., Tan, Q., Feng, M., An, J., Qu, Y., Zhang, Y., Jiang, M., 2018. Characteristics, source apportionment and contribution of vocs to ozone formation in wuhan, central China. *Atmos. Environ.* 192, 55–71. <https://doi.org/10.1016/j.atmosenv.2018.08.042>.
- Hwa, M.Y., Hsieh, C.C., Wu, T.C., Chang, L.F.W., 2002. Real-world vehicle emissions and vocs profile in the taipei tunnel located at taiwan taipei area. *Atmos. Environ.* 36, 1993–2002. [https://doi.org/10.1016/S1352-2310\(02\)00148-6](https://doi.org/10.1016/S1352-2310(02)00148-6).
- Jia, C., Mao, X., Huang, T., Liang, X., Wang, Y., Shen, Y., Jiang, W., Wang, H., Bai, Z., Ma, M., Yu, Z., Ma, J., Gao, H., 2016. Non-methane hydrocarbons (nmhc)s and their contribution to ozone formation potential in a petrochemical industrialized city, northwest China. *Atmos. Res.* 169, 225–236. <https://doi.org/10.1016/j.atmosres.2015.10.006>.
- Jobson, B.T., Berkowitz, C.M., Kuster, W.C., Goldan, P.D., Williams, E.J., Fesenfeld, F.C., Apel, E.C., Karl, T., Lonneman, W.A., Riemer, D., 2005. Hydrocarbon source signatures in houston, Texas: influence of the petrochemical industry. *J. Geophys. Res.: Atmos.* 109. <https://doi.org/10.1029/2004JD004887>.
- Jobson, B.T., Parrish, D.D., Goldan, P., Kuster, W., Fehsenfeld, F.C., Blake, D.R., Blake, N.J., Niki, H., 1998. Spatial and temporal variability of nonmethane hydrocarbon mixing ratios and their relation to photochemical lifetime. *J. Geophys. Res.: Atmos.* 103, 13557–13567. <https://doi.org/10.1029/97JD01715>.
- Kesselmeier, J., Staudt, M., 1999. Biogenic volatile organic compounds (voc): an overview on emission, physiology and ecology. *J. Atmos. Chem.* 33, 23–88. <https://doi.org/10.1023/A:1006127516791>.
- Khoder, M., 2007. Ambient levels of volatile organic compounds in the atmosphere of greater cairo. *Atmos. Environ.* 41, 554–566. <https://doi.org/10.1016/j.atmosenv.2006.08.051>.
- Klimont, Z., Streets, D.G., Gupta, S., Cofala, J., Lixin, F., Ichikawa, Y., 2002.

- Anthropogenic emissions of non-methane volatile organic compounds in China. *Atmos. Environ.* 36, 1309–1322. [https://doi.org/10.1016/S1352-2310\(01\)00529-5](https://doi.org/10.1016/S1352-2310(01)00529-5).
- Leuchner, M., Rappenglück, B., 2010. VOC source-receptor relationships in Houston during Texas-ii. *Atmos. Environ.* 44, 4056–4067. <https://doi.org/10.1016/j.atmosenv.2009.02.029>.
- Li, B., Ho, S.S.H., Gong, S., Ni, J., Li, H., Han, L., Yang, Y., Qi, Y., Zhao, D., 2019. Characterization of VOCs and their related atmospheric processes in a central Chinese city during severe ozone pollution periods. *Atmos. Chem. Phys.* 19, 617–638. <https://doi.org/10.5194/acp-19-617-2019>.
- Li, J., Zhai, C., Yu, J., Liu, R., Li, Y., Zeng, L., Xie, S., 2018. Spatiotemporal variations of ambient volatile organic compounds and their sources in Chongqing, a mountainous megacity in China. *Sci. Total Environ.* 627, 1442–1452. <https://doi.org/10.1016/j.scitotenv.2018.02.010>.
- Li, L., Xie, S., Zeng, L., Wu, R., Li, J., 2015. Characteristics of volatile organic compounds and their role in ground-level ozone formation in the Beijing-Tianjin-Hebei region, China. *Atmos. Environ.* 113, 247–254. <https://doi.org/10.1016/j.atmosenv.2015.05.021>.
- Li, M., Liu, H., Geng, G., Hong, C., Liu, F., Song, Y., Tong, D., Zheng, B., Cui, H., Man, H., Zhang, Q., He, K., 2017. Anthropogenic emission inventories in China: a review. *Nat. Sci. Rev.* 4, 834–866. <https://doi.org/10.1093/nsr/nwx150>.
- Ling, Z., Guo, H., Cheng, H., Yu, Y., 2011. Sources of ambient volatile organic compounds and their contributions to photochemical ozone formation at a site in the Pearl River Delta, southern China. *Environ. Pollut.* 159, 2310–2319. <https://doi.org/10.1016/j.envpol.2011.05.001>. Nitrogen Deposition. (Critical Loads and Biodiversity).
- Li, B., Cheng, Y., Zhou, M., Liang, D., Dai, Q., Wang, L., Jin, W., Zhang, L., Ren, Y., Zhou, J., Dai, C., Xu, J., Wang, J., Feng, Y., Zhang, Y., 2018. Effectiveness evaluation of temporary emission control action in 2016 in winter in Shijiazhuang, China. *Atmos. Chem. Phys.* 18, 7019–7039. <https://doi.org/10.5194/acp-18-7019-2018>.
- Liu, B., Liang, D., Yang, J., Dai, Q., Bi, X., Feng, Y., Yuan, J., Xiao, Z., Zhang, Y., Xu, H., 2016. Characterization and source apportionment of volatile organic compounds based on 1-year of observational data in Tianjin, China. *Environ. Pollut.* 218, 757–769. <https://doi.org/10.1016/j.envpol.2016.07.072>.
- Liu, B., Yang, J., Yuan, J., Wang, J., Dai, Q., Li, T., Bi, X., Feng, Y., Xiao, Z., Zhang, Y., Xu, H., 2017. Source apportionment of atmospheric pollutants based on the online data by using PMF and me2 models at a megacity, China. *Atmos. Res.* 185, 22–31. <https://doi.org/10.1016/j.atmosres.2016.10.023>.
- Liu, Y., Shao, M., Fu, L., Lu, S., Zeng, L., Tang, D., 2008. Source profiles of volatile organic compounds (VOCs) measured in China: Part i. *Atmos. Environ.* 42, 6247–6260. <https://doi.org/10.1016/j.atmosenv.2008.01.070>. pRIDE-PRD 2004 Campaign : Program of Regional Integrated Experiments on Air Quality over Pearl River Delta of China.
- Ma, Z., Xu, J., Quan, W., Zhang, Z., Lin, W., Xu, X., 2016. Significant increase of surface ozone at a rural site, north of eastern China. *Atmos. Chem. Phys.* 16, 3969–3977. <https://doi.org/10.5194/acp-16-3969-2016>.
- McCarthy, M.C., Aklilu, Y.A., Brown, S.G., Lyder, D.A., 2013. Source apportionment of volatile organic compounds measured in Edmonton, Alberta. *Atmos. Environ.* 81, 504–516. <https://doi.org/10.1016/j.atmosenv.2013.09.016>.
- Na, K., Kim, Y.P., 2001. Seasonal characteristics of ambient volatile organic compounds in Seoul, Korea. *Atmos. Environ.* 35, 2603–2614. [https://doi.org/10.1016/S1352-2310\(00\)00464-7](https://doi.org/10.1016/S1352-2310(00)00464-7).
- Nelson, P., Quigley, S., 1983. The m,p-xylene:ethylbenzene ratio, a technique for estimating hydrocarbon age in ambient atmospheres. *Atmos. Environ.* 17, 659–662. [https://doi.org/10.1016/0004-6981\(83\)90141-5](https://doi.org/10.1016/0004-6981(83)90141-5). 1967.
- Paatero, P., 1997. Least squares formulation of robust non-negative factor analysis. *Chemometr. Intell. Lab. Syst.* 37, 23–35. [https://doi.org/10.1016/S0169-7439\(96\)00044-5](https://doi.org/10.1016/S0169-7439(96)00044-5).
- Paatero, P., Tapper, U., 1994. Positive matrix factorization: a nonnegative factor model with optimal utilization of error estimates of data values. *Environmetrics* 5, 111–126. <https://doi.org/10.1002/env.3170050203>.
- Piero, D.C., Brune, W.H., Monica, M., Hartwig, H., Robert, L., Xinrong, R., Troy, T., Mary Anne, C., Valerie, Y., Shepson, P.B., 2004. Missing OH reactivity in a forest: evidence for unknown reactive biogenic VOCs. *Science* 304, 722–725.
- Poulopoulos, S., Philippopoulos, C., 2000. Influence of MTBE addition into gasoline on automotive exhaust emissions. *Atmos. Environ.* 34, 4781–4786. [https://doi.org/10.1016/S1352-2310\(00\)00257-0](https://doi.org/10.1016/S1352-2310(00)00257-0).
- Pusede, S., Steiner, A., Cohen, R., 2015. Temperature and recent trends in the chemistry of continental surface ozone. *Chem. Rev.* 115, 3898–3918. <https://doi.org/10.1021/cr5006815>.
- Pusede, S.E., Cohen, R.C., 2012. On the observed response of ozone to NO_x and VOC reactivity reductions in San Joaquin Valley California 1995–resent. *Atmos. Chem. Phys.* 12, 8323–8339. <https://doi.org/10.5194/acp-12-8323-2012>.
- Pusede, S.E., Gentner, D.R., Wooldridge, P.J., Browne, E.C., Rollins, A.W., Min, K.E., Russell, A.R., Thomas, J., Zhang, L., Brune, W.H., Henry, S.B., DiGangi, J.P., Keutsch, F.N., Harrold, S.A., Thornton, J.A., Beaver, M.R., St Clair, J.M., Wennberg, P.O., Sanders, J., Ren, X., VandenBoer, T.C., Markovic, M.Z., Guha, A., Weber, R., Goldstein, A.H., Cohen, R.C., 2014. On the temperature dependence of organic reactivity, nitrogen oxides, ozone production, and the impact of emission controls in San Joaquin Valley, California. *Atmos. Chem. Phys.* 14, 3373–3395. <https://doi.org/10.5194/acp-14-3373-2014>.
- Romer, P.S., Duffey, K.C., Wooldridge, P.J., Edgerton, E., Baumann, K., Feiner, P.A., Miller, D.O., Brune, W.H., Koss, A.R., de Gouw, J.A., Misztal, P.K., Goldstein, A.H., Cohen, R.C., 2018. Effects of temperature-dependent NO_x emissions on continental ozone production. *Atmos. Chem. Phys.* 18, 2601–2614. <https://doi.org/10.5194/acp-18-2601-2018>.
- Rubin, J.I., Kean, A.J., Harley, R.A., Millet, D.B., Goldstein, A.H., 2006. Temperature dependence of volatile organic compound evaporative emissions from motor vehicles. *J. Geophys. Res.: Atmos.* 111. <https://doi.org/10.1029/2005JD006458>.
- Seila, R.L., Main, H.H., Arriaga, J.L., V, G.M., Ramadan, A.B., 2001. Atmospheric volatile organic compound measurements during the 1996 Paso del Norte ozone study. *Sci. Total Environ.* 276, 153–169. [https://doi.org/10.1016/S0048-9697\(01\)00777-X](https://doi.org/10.1016/S0048-9697(01)00777-X).
- Shao, P., An, J., Xin, J., Wu, F., Wang, J., Ji, D., Wang, Y., 2016. Source apportionment of VOCs and the contribution to photochemical ozone formation during summer in the typical industrial area in the Yangtze River Delta, China. *Atmos. Res.* 176–177, 64–74. <https://doi.org/10.1016/j.atmosres.2016.02.015>.
- Singh, R.B., Sloan, J.J., 2006. A high-resolution NO_x emission factor model for North American motor vehicles. *Atmos. Environ.* 40, 5214–5223. <https://doi.org/10.1016/j.atmosenv.2006.04.012>.
- Song, C., He, J., Wu, L., Jin, T., Chen, X., Li, R., Ren, P., Zhang, L., Mao, H., 2017a. Health burden attributable to ambient PM_{2.5} in China. *Environ. Pollut.* 223, 575–586. <https://doi.org/10.1016/j.envpol.2017.01.060>.
- Song, C., Liu, Y., Sun, S., Sun, L., Zhang, Y., Ma, C., Peng, J., Li, Q., Zhang, J., Dai, Q., Liu, B., Wang, P., Zhang, Y., Wang, T., Wu, L., Hu, M., Mao, H., 2018. Vehicular volatile organic compounds (VOCs)-NO_x-CO emissions in a tunnel study in northern China: emission factors, profiles, and source apportionment. *Atmos. Chem. Phys. Discuss.* 2018, 1–38. <https://doi.org/10.5194/acp-2018-387>.
- Song, C., Wu, L., Xie, Y., He, J., Chen, X., Wang, T., Lin, Y., Jin, T., Wang, A., Liu, Y., Dai, Q., Liu, B., Wang, Y., Mao, H., 2017b. Air pollution in China: status and spatio-temporal variations. *Environ. Pollut.* 227, 334–347. <https://doi.org/10.1016/j.envpol.2017.04.075>.
- Song, Y., Shao, M., Liu, Y., Lu, S., Kuster, W., Goldan, P., Xie, S., 2007. Source apportionment of ambient volatile organic compounds in Beijing. *Environ. Sci. Technol.* 41, 4348–4353. <https://doi.org/10.1021/es0625982>.
- Steinbacher, M., Dommelen, J., Ordonez, C., Reimann, S., Grüebler, F.C., Staehelin, J., Prevot, A.S.H., 2005. Volatile organic compounds in the Po basin. part a: anthropogenic VOCs. *J. Atmos. Chem.* 51, 271–291. <https://doi.org/10.1007/s10874-005-3576-1>.
- Steiner, A.L., Davis, A.J., Sillman, S., Owen, R.C., Michalak, A.M., Fiore, A.M., 2010. Observed suppression of ozone formation at extremely high temperatures due to chemical and biophysical feedbacks. *Proc. Natl. Acad. Sci. Unit. States Am.* 107, 19685–19690. <https://doi.org/10.1073/pnas.1008336107>.
- Sun, Y., Jiang, Q., Wang, Z., Fu, P., Li, J., Yang, T., Yin, Y., 2014. Investigation of the sources and evolution processes of severe haze pollution in Beijing in January 2013. *J. Geophys. Res.: Atmos.* 119, 4380–4398. <https://doi.org/10.1002/2014JD021641>.
- Tsai, W.Y., Chan, L.Y., Blake, D.R., Chu, K.W., 2006. Vehicular fuel composition and atmospheric emissions in South China: Hong Kong, Macau, Guangzhou, and Zhuhai. *Atmos. Chem. Phys.* 6, 3281–3288. <https://doi.org/10.5194/acp-6-3281-2006>.
- Wang, B., Shao, M., Lu, S.H., Yuan, B., Zhao, Y., Wang, M., Zhang, S.Q., Wu, D., 2010. Variation of ambient non-methane hydrocarbons in Beijing city in summer 2008. *Atmos. Chem. Phys.* 10, 5911–5923. <https://doi.org/10.5194/acp-10-5911-2010>.
- Wang, G., Cheng, S., Wei, W., Zhou, Y., Yao, S., Zhang, H., 2016. Characteristics and source apportionment of VOCs in the suburban area of Beijing, China. *Atmos. Pollut. Res.* 7, 711–724. <https://doi.org/10.1016/j.apr.2016.03.006>.
- Wang, H., Chen, C., Wang, Q., Huang, C., Su, L., Huang, H., Lou, S., Zhou, M., Li, L., Qiao, L., Wang, Y., 2013. Chemical loss of volatile organic compounds and its impact on the source analysis through a two-year continuous measurement. *Atmos. Environ.* 80, 488–498. <https://doi.org/10.1016/j.atmosenv.2013.08.040>.
- Wang, M., Shao, M., Chen, W., Yuan, B., Lu, S., Zhang, Q., Zeng, L., Wang, Q., 2014. A temporally and spatially resolved validation of emission inventories by measurements of ambient volatile organic compounds in Beijing, China. *Atmos. Chem. Phys.* 14, 5871–5891. <https://doi.org/10.5194/acp-14-5871-2014>.
- Wang, Y., Zhang, X., Draxler, R.R., 2009. TrajStat: GIS-based software that uses various trajectory statistical analysis methods to identify potential sources from long-term air pollution measurement data. *Environ. Model. Softw.* 24, 938–939. <https://doi.org/10.1016/j.envsoft.2009.01.004>.
- Watson, J.G., Chow, J.C., Fujita, E.M., 2001. Review of volatile organic compound source apportionment by chemical mass balance. *Atmos. Environ.* 35, 1567–1584. [https://doi.org/10.1016/S1352-2310\(00\)00461-1](https://doi.org/10.1016/S1352-2310(00)00461-1).
- Wei, W., Cheng, S., Li, G., Wang, G., Wang, H., 2014. Characteristics of volatile organic compounds (VOCs) emitted from a petroleum refinery in Beijing, China. *Atmos. Environ.* 89, 358–366. <https://doi.org/10.1016/j.atmosenv.2014.01.038>.
- Wu, R., Xie, S., 2017. Spatial distribution of ozone formation in China derived from emissions of speciated volatile organic compounds. *Environ. Sci. Technol.* 51, 2574–2583. <https://doi.org/10.1021/acs.est.6b03634>.
- Yuan, B., Shao, M., Lu, S., Wang, B., 2010. Source profiles of volatile organic compounds associated with solvent use in Beijing, China. *Atmos. Environ.* 44, 1919–1926. <https://doi.org/10.1016/j.atmosenv.2010.02.014>.
- Yuan, Z., Hon, L.A.K., Shao, M., L.P.K., Liu, S., Zhu, T., 2009. Source analysis of volatile organic compounds by positive matrix factorization in urban and rural environments in Beijing. *J. Geophys. Res.: Atmos.* 114. <https://doi.org/10.1029/2008JD011190>.
- Yue, T., Yue, X., Chai, F., Hu, J., Lai, Y., He, L., Zhu, R., 2017. Characteristics of volatile organic compounds (VOCs) from the evaporative emissions of modern passenger cars. *Atmos. Environ.* 151, 62–69. <https://doi.org/10.1016/j.atmosenv.2016.12.008>.
- Zhang, Q., Wu, L., Fang, X., Liu, M., Zhang, J., Shao, M., Lu, S., Mao, H., 2018a. Emission factors of volatile organic compounds (VOCs) based on the detailed vehicle classification in a tunnel study. *Sci. Total Environ.* 624, 878–886. <https://doi.org/10.1016/j.scitotenv.2017.12.171>.
- Zhang, R., Jing, J., Tao, J., Hsu, S.C., Wang, G., Cao, J., Lee, C.S.L., Zhu, L., Chen, Z., Zhao, Y., Shen, Z., 2013a. Chemical characterization and source apportionment of PM_{2.5} in Beijing: seasonal perspective. *Atmos. Chem. Phys.* 13, 7053–7074. <https://doi.org/10.5194/acp-13-7053-2013>.
- Zhang, Y., Wang, X., Zhang, Z., L, S., Shao, M., Lee, F.S., Yu, J., 2013b. Species profiles and normalized reactivity of volatile organic compounds from gasoline evaporation

- in China. *Atmos. Environ.* 79, 110–118. <https://doi.org/10.1016/j.atmosenv.2013.06.029>.
- Zhang, Y., Yang, W., Simpson, I., Huang, X., Yu, J., Huang, Z., Wang, Z., Zhang, Z., Liu, D., Huang, Z., Wang, Y., Pei, C., Shao, M., Blake, D.R., Zheng, J., Huang, Z., Wang, X., 2018b. Decadal changes in emissions of volatile organic compounds (vocs) from on-road vehicles with intensified automobile pollution control: case study in a busy urban tunnel in south China. *Environ. Pollut.* 233, 806–819. <https://doi.org/10.1016/j.envpol.2017.10.133>.
- Zhang, Z., Zhang, Y., Wang, X., L, S., Huang, Z., Huang, X., Yang, W., Wang, Y., Zhang, Q., 2016. Spatiotemporal patterns and source implications of aromatic hydrocarbons at six rural sites across China's developed coastal regions. *J. Geophys. Res.: Atmos.* 121, 6669–6687. <https://doi.org/10.1002/2016JD025115>.
- Zhao, C., Wang, Y., Zeng, T., 2009. East China plains: a basin of ozone pollution. *Environ. Sci. Technol.* 43, 1911–1915. <https://doi.org/10.1021/es8027764>.
- Zhao, S., Yu, Y., Qin, D., Yin, D., Du, Z., Li, J., Dong, L., He, J., Li, P., 2019. Measurements of submicron particles vertical profiles by means of topographic relief in a typical valley city, China. *Atmos. Environ.* 199, 102–113. <https://doi.org/10.1016/j.atmosenv.2018.11.035>.
- Zhao, S., Yu, Y., Yin, D., He, J., Liu, N., Qu, J., Xiao, J., 2016. Annual and diurnal variations of gaseous and particulate pollutants in 31 provincial capital cities based on in situ air quality monitoring data from China national environmental monitoring center. *Environ. Int.* 86, 92–106. <https://doi.org/10.1016/j.envint.2015.11.003>.
- Zheng, H., Kong, S., Xing, X., Mao, Y., Hu, T., Ding, Y., Li, G., Liu, D., Li, S., Qi, S., 2018. Monitoring of volatile organic compounds (vocs) from an oil and gas station in northwest China for 1 year. *Atmos. Chem. Phys.* 18, 4567–4595. <https://doi.org/10.5194/acp-18-4567-2018>.
- Zhu, H., Wang, H., Jing, S., Wang, Y., Cheng, T., Tao, S., Lou, S., Qiao, L., Li, L., Chen, J., 2018. Characteristics and sources of atmospheric volatile organic compounds (vocs) along the mid-lower yangtze river in China. *Atmos. Environ.* 190, 232–240. <https://doi.org/10.1016/j.atmosenv.2018.07.026>.
- Zong, R., Yang, X., Wen, L., Xu, C., Zhu, Y., Chen, T., Yao, L., Wang, L., Zhang, J., Yang, L., Wang, X., Shao, M., Zhu, T., Xue, L., Wang, W., 2018. Strong ozone production at a rural site in thenorth China plain: mixed effects of urban plumesand biogenic emissions. *J. Environ. Sci.* 71, 261–270. <https://doi.org/10.1016/j.jes.2018.05.003>.
- Zou, Y., Deng, X.J., Zhu, D., Gong, D.C., Wang, H., Li, F., Tan, H.B., Deng, T., Mai, B.R., Liu, X.T., Wang, B.G., 2015. Characteristics of 1 year of observational data of vocs, no_x and O₃ at a suburban site in guangzhou, China. *Atmos. Chem. Phys.* 15, 6625–6636. <https://doi.org/10.5194/acp-15-6625-2015>.